SECTION III

PUBLISHED PAPERS
IN
JOURNALS
AND
CONFERENCE PROCEEDINGS

(JULY 1980-JUNE 1981)

Comparison of $^{24,25,26}Mg(p,n)^{24,25,26}Al$ Cross Sections with Giant $M1$ Strength

U. E. P. Berg,[a] Sam M. Austin, R. DeVito, A. I. Galonsky, and W. A. Sterrenburg
Cyclotron Laboratory and Physics Department, Michigan State University, East Lansing, Michigan 48824
(Received 16 January 1980)

Cross sections for the $^{24,25,26}Mg(p,n)^{24,25,26}Al$ reaction have been measured at 35 MeV. The strengths of the larger spin-isospin–flip transitions correspond surprisingly well with the matrix elements of the analogous giant $M1$ transitions.

PACS numbers: 25.40.Ep, 24.30.Cz, 27.30.+t

While substantial $M1$ strength has been found in the light nuclei, much less is known about its location for $A > 40$. In these heavier nuclei the transition strength appears to be spread over a wide range of excitation and fragmented among many levels, strongly reducing the sensitivity of the usual experimental techniques. Resonance fluorescence encounters background and statistical limitations and is, of course, useful only for bound states. Backward-angle electron scattering is hindered by increasing distortion effects which must be evaluated in a model-dependent fashion and by an intense background of $M2$ transitions. For example, not more than 15% of the predicted strength has been located in ^{90}Zr in spite of a serious experimental effort. It is then useful to search for other experimental probes which, while perhaps less precise, are more sensitive or selective. The (p,n) reaction at $E_p > 30$ MeV shows promise in this regard. For example, there is convincing evidence[2] that the reaction $^{90}Zr(p,n)^{90}Nb$ at 45 MeV strongly excites analogs of $M1$ strength in ^{90}Zr.

For the charge-exchange probe to provide quantitative rather than only qualitative information one needs, given the present state of art, to calibrate it in an empirical fashion. We present in this Letter the first systematic study of the relationship between $M1$ strength and (p,n) reactions at energies where the reaction mechanism is reasonably well understood, and for nuclei where individual states can be resolved and detailed electromagnetic information is available. Our data for the $^{24,25,26}Mg(p,n)^{24,25,26}Al$ reactions at $E_p = 35$ MeV yield a total of 16 correspondences between cross sections and $M1$ matrix elements $[B(M1)]$ of which all but two are in agreement within the uncertainties. This surprisingly strong correlation lends some confidence to the idea that studies of heavier nuclei with the (p,n) interaction at high energies will yield quantitative results on the distribution of $M1$ strength.

That one can use charge exchange reactions to search for $M1$ strength lies in the similarity of the operator for the two processes. If one neglects the isoscalar part of the $M1$ operator, which is an order of magnitude smaller than the isovector part, the isovector $M1$ operator and the central (p,n) spin-isospin–flip (SISF) operator are identical in the spin-isospin space of the valence nucleons, containing $\vec{\sigma}$ and $\vec{\tau}$ which flip spin and isospin, respectively. One therefore expects strong $M1$ transitions to be strong in (p,n) reactions. There will not be a perfect match of $B(M1)$ and $\sigma(p,n)$ because the radial parts of the operators are different and because of the current $(\vec{j})$ term in the $M1$ operator, but they will bear a strong similarity. Since, e.g., absorption of magnetic dipole radiation leads to strong 1^+, $T = 1$ $[T_3 = \frac{1}{2}(N-Z) = +1]$ states near 10 MeV in ^{26}Mg we expect strong (p,n) transitions to their analogs in ^{26}Al with $J^\pi = 1^+$, $T = 1$ $(T_3 = 0)$ at about 10 MeV above the isobaric analog of the ^{26}Mg ground state.

The (p,n) studies were performed with 35-MeV protons from the Michigan State University cyclotron. The beam-burst interval was chosen to allow the observation of neutron energies between 14 and 30 MeV. Angular distributions from 7° to 120° were taken with a beam-swinger system[3] and a 22.48 m flight path. All three Mg targets were 5.0-mg/cm^2 foils isotopically enriched to 99.5% in $^{24,25,26}Mg$, respectively. The energy resolution was 180 keV for 30-MeV neutrons [from the isobaric analog state (IAS) in $^{25,26}Al$] and 90 keV for 20-MeV neutrons (from the ground state in ^{24}Al, $Q = -14.665$ MeV). The spectra show strong, well-resolved transitions even at excitation energies near 10 MeV (see Fig. 1).

To identify the SISF transitions, we used mainly the following criteria: The angular distributions should be similar to those for known SISF transitions to 1^+ states; excitation energies of analog states in the Al isotopes should correspond to the known excitation energies of the parent magnetic dipole states in the Mg nuclei.

Figure 2 shows the angular distribution of the $^{26}Mg(p,n)$ cross section to the first 1^+ state in

Coalescence of Light Particles in the Reaction $^{16}O+^{238}U$ at 315 MeV

T. C. Awes, C. K. Gelbke, and G. Poggi[a]
Cyclotron Laboratory, Michigan State University, East Lansing, Michigan 48824

and

B. B. Back and B. Glagola
Chemistry Division, Argonne National Laboratory, Argonne, Illinois 60439

and

H. Breuer and V. E. Viola, Jr.,
Departments of Physics and Chemistry, University of Maryland, College Park, Maryland 20742

and

T. J. M. Symons
Nuclear Science Division, Lawrence Berkeley Laboratory, Berkeley, California 94720
(Received 2 June 1980)

The energy spectra of light particles (p,d,t) produced in ^{16}O-induced reactions on ^{238}U at 315 MeV can be rather well described by thermal distributions in a rest frame that moves with about half the beam velocity. The energy spectra of deuterons and tritons can be related to the proton energy spectra by a coalescence model that incorporates Coulomb effects.

PACS numbers: 25.70.Fg, 25.70.Bc

It has been pointed out[1-3] that the production of composite light particles contains important information on the reaction mechanism of heavy-ion–induced reactions. At relativistic energies ($E/A \gtrsim 200$ MeV/u), the emission of composite light particles has been shown to relate to the emission of protons via the coalscence model.[4,5] Up to the present, however, the coalescence relation has not been tested for heavy-ion–induced reactions at nonrelativistic energies. In this Letter we investigate ^{16}O-induced reactions on ^{238}U at 20 MeV/u and demonstrate the validity of a generalized coalescence relation which takes into account the effect of Coulomb repulsion from the target nucleus. The validity of the coalescence relation at this low energy renders possible a coherent study of composite–light-particle production with use of a single concept over a wide range of energies from a few tens to a few thousands of MeV/u.

The experiment was performed at the 88-in. cyclotron of the Lawrence Berkeley Laboratory. A self-supporting, metallic ^{238}U target of approximately 500 $\mu g/cm^2$ areal density was bombarded with $^{16}O^{6+}$ ions of 315 MeV. Correlated fission fragments were recorded in two position-sensitive solid-state detectors. Coincident light particles were measured with four ΔE-E telescopes each consisting of a 400-μm surface-barrier detector and a 3-in.-thick NaI detector. These tele-

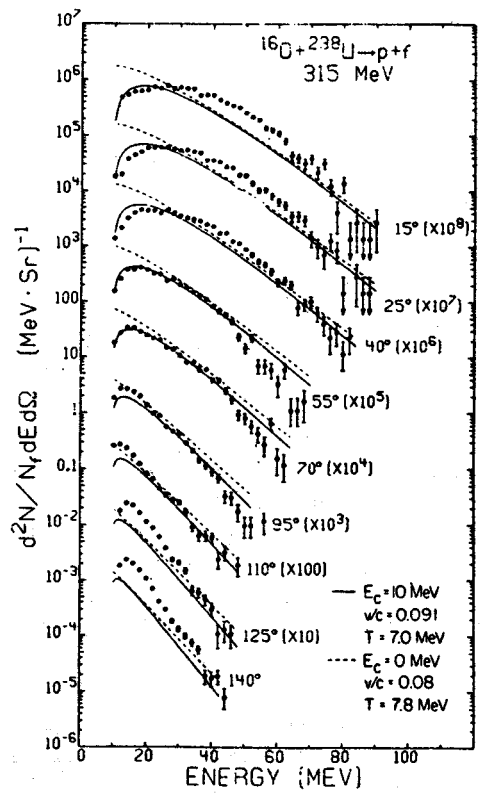

FIG. 1. Energy spectra of protons detected in the reaction $^{238}U(^{16}O,pf)$ at 315 MeV. The curves have been calculated with Eq. (1) of the text.

Q-Value Systematics for Isovector Giant Resonances Excited by (p,n) Reactions on Zr, Nb, Mo, Sn, and Pb Isotopes

W. A. Sterrenburg, Sam M. Austin, R. P. DeVito, and Aaron Galonsky
Cyclotron Laboratory, Michigan State University, East Lansing, Michigan 48824
(Received 7 July 1980)

The (p,n) reaction at 45 MeV is used to study two broad peaks found previously with the target ^{90}Zr. They have now been observed with all but one of seventeen targets from ^{90}Zr to ^{208}Pb. Energy systematics favor the conclusion that these peaks are antianalogs of the giant $M1$ and $E1$ resonances in the target nucleus. The first experimental determinations of T, $T-1$ splittings of the giant $E1$ resonance are reported. Their low values in comparison to T, $T+1$ splittings observed previously can be interpreted as due to a tensor part of the effective isospin potential.

PACS numbers: 25.40.Ep, 24.30.Cz

Many studies with (p,n) reactions have focused on the most prominent feature in the neutron spectra, i.e., on the isobaric analogs of ground states (IAS). In the (p,n) reaction on ^{90}Zr at a bombarding energy of 45 MeV two other features were observed.[1] The first was a peak about 4 MeV wide not far above the IAS which was interpreted as the $T-1$ component (T =target isospin) of the predicted[2] giant Gamow-Teller (GT) or spin-flip transition. Alternatively, this peak may be thought of as the antianalog of a giant magnetic dipole state[1] in the target, ^{90}Zr. The other feature, another cross-section enhancement, located about 10 MeV higher in excitation energy, was observed with the reaction ^{90}Zr(^{3}He,t) at 130 MeV and confirmed in 45-MeV (p,n) spectra[3] and in (p,n) data at higher energies.[4] It was suggested by Marty[5] that this peak is the $T-1$ component of the giant (electric) dipole resonance. A charge-exchange reaction, such as the (p,n) reaction, is the only way to excite such $T-1$ strength.

Thus far these phenomena have been observed only in ^{90}Zr. To determine whether they occur more generally we have obtained[6] (p,n) spectra for seventeen nuclei ($^{90\text{-}92,\,94,\,96}$Zr, ^{93}Nb, $^{94,\,96\text{-}98,\,100}$Mo, $^{112,\,116,\,120,\,122,\,124}$Sn, and ^{208}Pb) at E_p =45 MeV. With one exception we find the two peaks for all nuclei studied. In addition, the systematic variation of the location of these peaks is strong evidence for their interpretation as the antianalogs, with isospin $T-1$, of the giant $M1$ and $E1$ excitations in the parent nuclei. These data represent the first observation of GT $E1$ strength outside of ^{90}Zr and provide for the first time a substantial body of data for testing theories of the location and isospin splitting of these resonances. The relevant states of a target and its isobaric daughter nucleus are illustrated in Fig. 1.

The (p,n) studies were performed with the beam-swinger neutron time-of-flight system at Michigan State University.[7] All targets were isotopically enriched, most to > 95%, and had thicknesses of 1–10 mg/cm^2. The neutron detector was a cylinder (12.7 cm diam×7.6 cm thick) of NE-213 liquid scintillator placed 7 m from the target.

Figure 2 shows neutron time-of-flight spectra for four Sn isotopes. In addition to the IAS at about 31 MeV neutron energy and the sharp γ-ray peak leaking through the pulse-shape discriminator, two broad peaks are clearly visible in all four spectra. The smooth curves are fits through

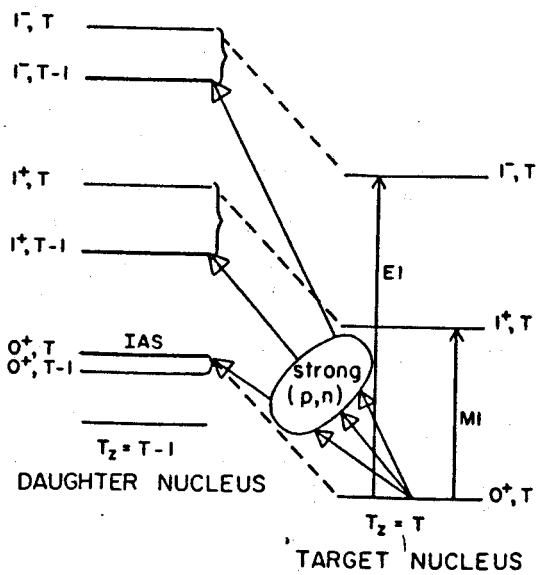

FIG. 1. Some states of the target nucleus ($T_z = T$) and their analogs (isospin = T) and antianalogs (isospin = $T-1$) in the $T_z = T-1$ nucleus resulting from a (p,n) reaction. The target states are the ground state and the $M1$ and $E1$ giant resonant states. Isospin geometry strongly favors the three transitions indicated.

Pauli Suppression of Momentum Fluctuations

G. Bertsch
Cyclotron Laboratory and Department of Physics, Michigan State University, East Lansing, Michigan 48824
(Received 23 October 1980)

Pauli correlations are shown to be important in interpreting the momentum distribution of nuclear fragments formed in high-energy heavy-ion collisions.

PACS numbers: 24.10.-i, 25.70.-z, 24.90.+d

The fast fragments emerging from relativistic heavy-ion collisions have a narrow momentum distribution with a Gaussian shape.[1] This distribution is described with some success by the independent-particle model.[2] However, the independent-particle model ignores all correlations beyond the purely kinematical ones. The Pauli correlations, in particular, are very important and reduce the dispersions in measurements of one-body operators. I will show that this is also the case for the momentum operator, and that inclusion of these correlations improves agreement between theory and experiment.

I first recall Goldhaber's derivation of the momentum dispersion in the independent-particle model.[2] One can pick F nucleons from the projectile to make the fragment, and calculate the expectation of the squared momentum of these nucleons in the projectile initial state. In the frame of the projectile, this yields a dispersion

$$\sigma^2 = \langle [\sum_i^F p_z(i)]^2 \rangle = F\langle p_z^2(1)\rangle + F(F-1)\langle p_z(1)p_z(2)\rangle. \quad (1)$$

The first term in Eq. (1) can be estimated in the Fermi-gas model as[3]

$$\langle p_z^2\rangle = \tfrac{1}{5} p_F^2,$$

where p_F is the Fermi momentum, as measured, for example, by inelastic electron scattering.

To calculate the second term in Eq. (1), Goldhaber uses the fact that the total momentum of the original nucleus is zero:

$$\langle [\sum_i^A p_z(i)]^2 \rangle = A\langle p_z^2(1)\rangle + A(A-1)\langle p_z(1)p_z(2)\rangle = 0. \quad (2)$$

Combining Eqs. (1) and (2), I find, for the momentum dispersion,

$$\sigma^2 = \langle (\sum_i^F p_i)^2 \rangle = [F(A-F)/(A-1)](\tfrac{1}{5} p_F^2). \quad (3)$$

Experimentally, with ^{40}Ar projectiles, it is found that the dispersion σ^2 is 31% lower than predicted by Eq. (3).[4]

I will improve this model by treating the correlation terms involving identical nucleons more carefully. Qualitatively, one expects that there is a large anticorrelation between the momenta of two identical particles when they are close together in coordinate space. To calculate the effect, one needs to include some spatial details of the measurement process. The experiment measures the momentum in the z direction when a region of matter delineated in the transverse directions is removed from the projectile. Thus the operator acting on the nucleus has the form

$$\mathcal{O} = p_z f(x, y), \quad (4)$$

where $f = 0$ or 1 in the regions of the nucleus that are removed or remain in the fragment. The operator $\mathcal{O}^2$ can be easily evaluated in a determinantal wave function that is separable in Cartesian coordinates,

$$\psi = \mathcal{A} \prod_n^a \varphi_{n_x}(x)\varphi_{n_y}(y)\varphi_{n_z}(z). \quad (5)$$

Here $n \equiv (n_x, n_y, n_z)$ labels the quantum numbers of the occupied orbits, and the total number of orbits is a. The matrix elements are evaluated as

$$\langle\psi|\sum_i^a \mathcal{O}_i^2|\psi\rangle = \sum_n \langle n_x n_y|f|n_x n_y\rangle\langle n_z|p_z^2|n_z\rangle, \quad (6)$$

$$\langle\psi|\sum_{i\neq j}^{a(a-1)} \mathcal{O}_i\mathcal{O}_j|\psi\rangle = -\sum_{n\neq n'} \langle n_x n_y|f|n_x' n_y'\rangle^2\langle n_z|p_z|n_z'\rangle^2. \quad (7)$$

I also need to include the correlation between nonidentical nucleons. The complete expression for the momentum dispersion in a nucleus with four nucleons in each orbit, i.e., $A = 4a$, is given by

$$\langle\mathcal{O}^2\rangle = 4\langle\psi|\sum_i^a \mathcal{O}_i^2|\psi\rangle + 4\langle\psi|\sum_{i\neq j}^{a(a-1)} \mathcal{O}_i\mathcal{O}_j|\psi\rangle + 12a^2\langle\mathcal{O}_i\mathcal{O}_k\rangle_{\text{nonidentical}}. \quad (8)$$

Observation of $M1$ Strength by the Inelastic Scattering of 200-MeV Protons

N. Anantaraman, G. M. Crawley, and A. Galonsky
Cyclotron Laboratory, Michigan State University, East Lansing, Michigan 48824

and

C. Djalali, N. Marty, M. Morlet, A. Willis, and J.-C. Jourdain
Institut de Physique Nucléaire, F-91406 Orsay, France

(Received 9 March 1981)

A new resonance has been observed at very forward angles in the inelastic scattering of 200-MeV protons on ^{90}Zr, ^{92}Zr, and ^{94}Zr at an excitation energy around 8.8 MeV in each target. The excitation energy, angular distribution, and strength of this state suggest that it corresponds to the previously unseen giant $M1$ transition in the zirconium isotopes.

PACS numbers: 24.30.Cz, 25.40.Ep, 27.60.+j

The location of $M1$ strength in medium and heavy nuclei has been a long-standing and major problem in nuclear structure physics.[1] While various theoretical estimates[2,3] have indicated that $M1$ states should exist below 12 MeV excitation energy in nuclei with $A > 60$, little or no significant $M1$ strength has been observed. This strength has been searched for in both hadron,[4,5] and electron[6-8] inelastic scattering but so far without success. There has been some $M1$ strength reported[9] in ^{208}Pb and a mention[10] of strength observed in (e,e') on ^{90}Zr, which has not been substantiated by later measurements.[7]

In contrast, there has been observed in recent charge-exchange[11-17] experiments on more than twenty target nuclei, a broad resonance which is generally accepted as the giant Gamow-Teller (GT) resonance. This transition, in which $\Delta J^{\pi} = 1^{+}$, is successfully accounted for in terms of the shell model,[18] and the same considerations would predict appreciable strength for a giant $M1$ state in the target. Hence, we have the paradoxical situation that the transition to the $T_<$ state in the daughter nucleus has been observed many times, but the parent of the $T_>$ state has never been seen. The elusiveness of the parent state casts doubt upon the interpretation of the charge-exchange experiments. The present results resolve this paradox.

The GT peak, which is greatly enhanced at forward angles, is much stronger relative to the background at 120 MeV (Ref. 14) than at 45 MeV bombarding energy.[11] Its 1^{+} character has been established on the basis of excitation energy and the observed angular distributions. In addition to the broad bump observed in the reaction ^{90}Zr$(p,n)^{90}$Nb, about 3.6 MeV above the isobaric analog of the target ground state, a second smaller peak is indicated about 8.3 MeV above the isobaric analog state (IAS)[13,19] which also appears to have a predominantly $l = 0$ angular distribution. It has been suggested that this peak is the $T = 5$ $(T_>)$ component of the giant GT resonance. However, it is too weak and too close to the large $T = 4$ $(T_<)$ bump to be clearly separated from it.

These results implied that $M1$ strength might be observable in the parent nucleus with use of the (p,p') reaction. The expected excitation energy would be given by the difference between the energies of the IAS and the $T_>$ peak, viz. 8.3 MeV in ^{90}Zr. The GT peak in (p,n) reactions is more prominent at higher bombarding energies because the ratio of the spin-flip component, $V_{\sigma\tau}$, to the non-spin-flip component, V_{τ}, of the effective interaction increases with energy.[20-24] In the (p,p') reaction above 100 MeV, the same component, $V_{\sigma\tau}$, is mainly responsible for unnatural parity transitions such as $0^{+} \rightarrow 1^{+}$ at small momentum transfer. Since the reaction dynamics should be similar for (p,p') and (p,n) reactions at similar bombarding energies, 1^{+} states in (p,p') should also be excited mainly through an $l = 0$ transfer. These states should, therefore, show the same sharp forward peaking of the angular distribution which characterized the GT peak in the (p,n) reaction.

These considerations prompted a search for $M1$ strength in medium weight nuclei with use of the 201 MeV proton beam from the Orsay synchrocyclotron and a large magnetic spectrometer. The targets used were calcium (natural Ca; 15.0 mg/cm^2), ^{90}Zr (97.65% enriched; 18.9 mg/cm^2), ^{92}Zr (95.13% enriched; 25.4 mg/cm^2), and ^{94}Zr (98.6% enriched; 16.4 mg/cm^2). The particles were detected by two multiwire proportional counters[25] backed by two plastic scintillators. The

HIGH ENERGY PROTON EMISSION IN REACTIONS INDUCED BY 315 MeV ^{16}O IONS ☆

T.J.M. SYMONS, P. DOLL [1], M. BINI [2], D.L. HENDRIE, J. MAHONEY, G. MANTZOURANIS, D.K. SCOTT, K. Van BIBBER, Y.P. VIYOGI [3] and H.H. WIEMAN
Lawrence Berkeley Laboratory, University of California, Berkeley, CA 94720, USA

and

C.K. GELBKE
Physics Department, Michigan State University, East Lansing, MI 48824, USA

Received 3 July 1979

Inclusive proton spectra have been measured for the reaction ^{197}Au(^{16}O, p)X at 315 MeV. The data, which are consistent with emission from a moving source, are compared with the fireball model and with models of preequilibrium emission.

In this letter we report the measurement of inclusive proton spectra from the reaction of 315 MeV ^{16}O ions on a ^{197}Au target. The motivation for this work was provided by the growth of interest in high energy proton emission accompanying heavy ion collisions. At low energies ($E/A \leqslant 10$ MeV/nucleon) the emission of energetic light particles has been discussed in terms of break-up reactions [1], cascade calculations [2], preequilibrium models [3] and, more recently, hot spots [4] and jets [5,6]. At relativistic energies ($E/A \geqslant 200$ MeV/nucleon) the concept has emerged of a localized equilibrated source moving at a velocity midway between projectile and target residue, and quantitative descriptions of inclusive spectra have been possible in terms of the fireball [7] and firestreak [8] models. It is an important question to ask what happens to the concept of localization used in the fireball model as the bombarding energy is reduced. For example, it has been suggested [4] that this localization may persist in the form of hot spots on the nuclear surface. Nevertheless, it is clear that a transition must take place to mean field phenomena [9] and that the energy at which it occurs should be related to the relaxation time of nuclear matter. We find that at 20 MeV/nucleon, in the transition region between low and high energy processes [10,11], the fireball model gives a surprisingly good account of the observed spectra. Simultaneously, however, a description appears possible in terms of conventional low energy concepts.

The $^{16}O^{6+}$ beam from the Lawrence Berkeley Laboratory 88 inch Cyclotron was used to bombard a ^{197}Au target of 9.5 mg cm^{-2}. High energy protons were detected in a telescope consisting of 1 mm and 5 mm thick Si(Li) detectors, each of 5 cm diameter, and a 7.5 cm × 7.5 cm cylindrical NaI(Tl) detector. The detectors were mounted outside a sliding seal scattering chamber and viewed the target through a 0.002" Mylar window. A second telescope made up of a 200 μm Si surface barrier detector, a 5 mm Si(Li) detector and a veto detector, was mounted inside the scattering chamber and was used to measure low energy light particles. The detectors were calibrated up to 90 MeV proton energy with 45 MeV protons elastically scattered from ^{197}Au and polyethylene targets and also with protons produced in the ^{12}C(α, p)^{15}N reaction at inci-

☆ This work was supported by the Nuclear Physics Division of the Department of Energy.

[1] NATO Fellow. Permanent address: MPI, Heidelberg, Fed. Rep. Germany.

[2] NATO Fellow. On leave from University of Florence, Florence, Italy.

[3] IAEA Fellow. On deputation from BARC, Calcutta, India.

THE NUCLEAR DENSITY OF STATES IN THE SPACE OF NUCLEAR SHAPES

G. BERTSCH
Department of Physics, Michigan State University, East Lansing, MI 48824, USA

Received 2 June 1980

The density of states for the nuclear shape degrees of freedom are calculated in the Fermi gas model. For quadrupole deformations, the resulting formulas agree well with the properties of the deformed excited states of ^{16}O and ^{40}Ca. Application is also made to the inertia associated with the deformation coordinate. The inertia turns out to be much smaller than given by the weak coupling limit.

The nuclear shape degrees of freedom introduce a complexity into the density of states that has not been adequately characterized. In this note we will address the question of how dense the population of lowest states is in the space of nuclear shape degrees of freedom.

The lowest states may be defined by constrained Hartree–Fock calculations. For example, consider some particular shape degree of freedom parameterized by a coordinate y, with the Hartree–Fock states constrained to have a shape moment corresponding to y. Then the lowest state would lie on a set of parabolas as shown in fig. 1. Each parabola defines a different Hartree–Fock state, and the question is to determine the number of states per unit interval in y, dn/dy.

It is first necessary to understand how the nuclear wavefunction depends on deformation. For small changes in y, the Hartree–Fock state remains in the same parabola, and the transformation of the wavefunction is well described by a displacement field $u(r)$,

$$\psi_{y+\Delta y}(r_1, r_2, \ldots) = \psi_y(r_1 + \Delta y\, u, r_2 + \Delta y\, u, \ldots) . \quad (1)$$

Because it requires more energy to compress nuclear matter than to deform it, the transformation will be volume preserving, $\nabla \cdot u = 0$. For example, for quadrupole deformations of spherical nuclei, the displacement field will have the form [‡1]

$$u = \nabla r^2 P_2(\hat{r}) . \quad (2)$$

An important effect of the transformation (1) is to modify the local momentum of the nucleons according to [1]

$$p' = p \cdot (1 - \Delta y \nabla u) . \quad (3)$$

This results in a distortion of the Fermi surface. The extra kinetic energy of the distortion in fact provides the restoring force toward the equilibrium of the parabola.

The equilibrium is characterized by a spherical Fermi surface, and this provides the criterion for how much distortion is required to pass from one equilibrium y_1 to the next, y_2. On the average, a new minimum is possible when the volume of phase space in the distorted Fermi surface with $p > p_F$ exceeds $(2\pi)^3$, i.e.,

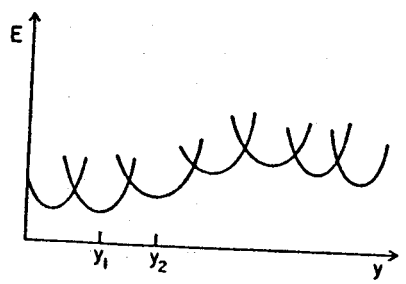

Fig. 1. Schematic picture of Hartree–Fock energy as a function of shape parameter.

[‡1] This may be seen from the Wigner representation of the density matrix, making a Taylor series expansion of u. Cf. ref. [1].

THE EFFECT OF THE NUCLEAR MEDIUM ON S-WAVE PION ABSORPTION*

D.O. RISKA and H. SARAFIAN
Department of Physics and National Superconducting Cyclotron Laboratory, Michigan State University, East Lansing, MI 48824, USA

Received 1 April 1980
Revised manuscript received 2 June 1980

It is shown that the effects of the nuclear medium on the pion propagator and the renormalization of the πNN interaction, described in terms of excitation of virtual isobar–hole pairs can enhance the predicted absorption rates for pions at threshold to values close to the empirical ones.

Recent attempts at explaining the empirical rates for nuclear pion absorption at threshold in terms of simple two-body rescattering mechanisms have led to underpredictions of the order 20–30% [1]. Similarly the predicted values for the main absorptive two-nucleon component of the S-wave pion-nucleus optical potential have also been considerably smaller than those suggested by optical model studies of pion atom data [1–4]. We shall here show that the effects of successive excitation of virtual isobar–hole pairs in the nuclear medium on the propagation of the rescattered meson, and on the P-wave πNN interaction, can enhance the predicted absorption rates by the amounts needed.

The absorption of S-wave pions at threshold is usually described in terms of the two-body rescattering mechanism illustrated in fig. 1a. Here the pion undergoes an initial S-wave scattering off one nucleon, and then propagates through the nucleus until absorbed on a second nucleon by the usual P-wave πNN interaction. The presence of the nuclear medium adds a self energy Π to the pion propagator and renormalizes the final P-wave interaction. These medium corrections are schematically indicated in fig. 1b.

* Research supported in part by the National Science Foundation.

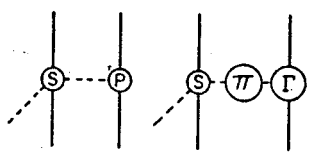

Fig. 1. S-wave pion absorption mechanism without (a) and with (b) medium effects.

For the pion self energy we employ the picture of Barshay, Brown and Rho [5] and Baym and Brown [6] which involves excitation of isobar–hole pairs. We shall use a similar description to obtain the πNN vertex renormalization, following the suggestion of Rho [7]. In this picture the pion self energy is made up of the single isobar hole pairs connected by the reduced isobar–hole interaction (R), with the single pion exchange contribution subtracted out, as illustrated in fig. 2.

The self energy contribution from the single isobar–hole pair is, with account of both time orderings of the Δ_{33} resonance,

$$\Pi_0 = -\frac{4}{9}\left(\frac{f_\Delta}{\mu}\right)^2 k^2 f_\pi^2(k)\rho\left(\frac{1}{D_1}+\frac{1}{D_2}\right) \qquad (1)$$

Here k is the pion momentum, μ the pion mass and ρ

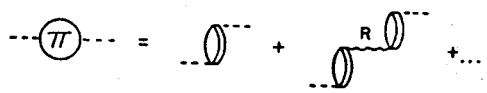

Fig. 2. Model for the pion self energy Π involving the reduced isobar–hole interaction R.

REDUCTION OF MAGNETIC AND TRANSVERSE ELECTRIC SCATTERING AMPLITUDES IN ^{207}Pb BY CORE POLARIZATION

I. HAMAMOTO [1,2]

Center for Theoretical Physics, Laboratory for Nuclear Science and Department of Physics, M.I.T., Cambridge, MA. 02139, USA

J. LICHTENSTADT [1,3]

Bates Linear Accelerator Center, Laboratory for Nuclear Science and Departmetn of Physics, M.I.T., Cambridge MA. 02139, USA

and

G.F. BERTSCH [4]

Department of Physics and Cyclotron Laboratory Michigan State University, East Lansing MI 38824, USA

Received 17 August 1980

It is shown that core-polarization causes a considerable reduction of the nuclear magnetization current at high momentum transfer irrespective of multipolarity. The reduction is consistent with the observed reduction of both magnetic and transverse electric form factors in the ^{207}Pb and ^{208}Pb nuclei. No corresponding systematic reduction is expected in the nuclear convection current.

In recent high resolution electron scattering experiments on ^{207}Pb [1,2] the low lying neutron hole excitations have been studied. It has been observed that there is a systematic reduction of the transverse scattering amplitude to about 55% of the single particle value, independent of the transition multipolarity and the momentum transfer investigated. Various mechanisms were suggested to explain this reduction. In this letter we present a calculation of the core polarization effect on the nuclear magnetization currents which accounts for a substantial part of this reduction in both magnetic and electric transitions. We use the same model [3] by which a similar reduction was obtained in the high spin transitions ($J^\pi = 12^-, 14^-$) in ^{208}Pb [4]. While in the latter only the first maxima of the magnetic form factors have been measured those of the low multipolarity transitions discussed here exhibit several peaks in the probed momentum transfer range and provide an opportunity to study the core polarization effect via electric and magnetic transitions with different multipolarities and different forms of wave functions involved.

The states discussed here are at 0.571 MeV ($3p_{1/2} \rightarrow 2f_{5/2}$), 0.899 MeV ($3p_{1/2} \rightarrow 3p_{3/2}$), 1.634 MeV ($3p_{1/2} \rightarrow 1i_{13/2}$), and at 2.340 MeV ($3p_{1/2} \rightarrow 2f_{7/2}$). In each of these the neutron-hole configuration (mentioned) is supposed to be the overwhelmingly predominant component in both the initial and final states (denoted by p_0 and p_1 respectively). Thus we estimate the core-polarization by perturbation. We obtain the following inhomogeneous equation [3,5,6] for the perturbed particle wave-function $X_{ph}(r)$:

$$\left[\frac{\hbar^2}{2m}\left(-\frac{d^2}{dr^2}+\frac{l_p(l_p+1)}{r^2}\right)+V(r)-(\epsilon_{p_1}-\epsilon_{p_0}+\epsilon_h)\right] \times rX_{ph}(r) = -rR_h(r)R_{p_0}(r)R_{p_1}(r)\sqrt{\frac{2\lambda+1}{2j_{p_0}+1}}(-1)^{j_{p_0}+j_{p_1}+\lambda}$$

[1] Supported in part by U.S. D.O.E. contract No. DE-AC0276 ER03069.

[2] Address after Sept. 1980: Nordita, Blegdamsvej 17, Copenhagen, Denmark.

[3] Address after Sept. 1980: Tel-Aviv University, Tel-Aviv, Israel.

[4] Supported in part by the National Science Foundation.

PROTON POLARIZABILITY IN THE MIT BAG MODEL ☆

P.C. HECKING and G.F. BERTSCH
Cyclotron Laboratory and Department of Physics, Michigan State University, East Lansing, MI 48824, USA

Received 15 December 1980

The polarizability of the proton is calculated in a simplified MIT bag model and compared with an analysis of Compton scattering. Qualitative agreement is obtained for the sum of the electric and magnetic polarizabilities, which is found to be within 30% of the experiment.

The determination of the electric and magnetic proton polarizabilities α and β from experiment and their connection with sum rules has been controversial for some time. The combination $\alpha+\beta$ is well determined by the sum rule [‡1]

$$\alpha+\beta=\frac{1}{2\pi^2}\int_0^\infty \frac{\sigma(\omega)}{\omega^2}\,d\omega = 14.1\pm 0.3\,. \tag{1}$$

The difference $\alpha-\beta$, however, is model dependent. Values of −9.7 [1] −6 [2] and +12.5 [3] have been obtained, depending on the type of dispersion relation and the channels taken into account. The most recent analysis [1] of Compton scattering at 80–110 MeV gives values

$$\alpha = 20\pm 1.1, \beta = -(6\pm 1.6)\,.$$

The authors of ref. [1] claim that dropping the ω^4 -terms in former analyses [4,5] has yielded incorrect values of $\alpha = 9\pm 2(10.7\pm 1.1)$ and $\beta = 2\pm 2(-0.7\pm 1.6)$, respectively.

In this work we calculate the polarizabilities in the MIT bag model [6,7]. This model has been very successful in the prediction of ground-state properties of hadrons; it is generally not quite so good for dynamical quantities, such as transition probabilities.

In a model of non-interacting quarks, the polarizabilities are given by:

$$\alpha = 2\sum_{j=1}^{3}\sum_{\lambda} e_j^2\,\frac{|\langle\phi_{0j}|\gamma_0 z|\phi_{\lambda j}\rangle|^2}{E_j^\lambda - E_j}, \tag{2a}$$

$$\beta = 2\sum_{j=1}^{3}\sum_{\lambda} e_j^2\,\frac{|\langle\phi_{0j}|\boldsymbol{\gamma}\cdot\tfrac{1}{2}(\hat{z}\times r)|\phi_{\lambda j}\rangle|^2}{E_j^\lambda - E_j}. \tag{2b}$$

Here $|\phi_{0j}\rangle$ and $|\phi_{\lambda j}\rangle$ are normalized single-quark wavefunctions, and γ_0 and $\boldsymbol{\gamma}$ are the usual Dirac matrices; $|\phi_{0j}\rangle$ is the $1s_{1/2}$ wavefunction of the nucleon ground state, and $|\phi_{\lambda j}\rangle$ are excited quark- or antiquark states. The charge of the jth quark is e_j. In the case of the proton, the sum over e_j reduces to $\Sigma_{j=1}^3 e_j^2 = e^2(\frac{1}{9}+\frac{4}{9}+\frac{4}{9}) = e^2$. The wavefunctions $|\phi_{0j}\rangle$ and $|\phi_{\lambda j}\rangle$ are assumed to be the same for all three quarks in a particular space-spin state. Only a few terms are important in the sum over the space-spin states $|\phi_{\lambda j}\rangle$. The 1p and 1s quark and antiquark states are taken into account. The other states lie further away in the energy spectrum, and thus give much smaller contributions. Of these, the $1p_{1/2}$, $1p_{3/2}$ quark and the $1s_{1/2}$ antiquark state contribute to the electric polarizability, whereas for the magnetic polarizability the intermediate states are the $1s_{1/2}$ quark and the $1p_{1/2}$, $1p_{3/2}$ antiquark. The antiquark contribution can be viewed as an exchange effect.

We use the same size bag for all states, and assume that the quarks have zero rest mass. Then the wavefunctions to be considered are:

☆ Work supported in part by NSF and DFG under contract He 1155/1.

‡1 α and β are given in units of 10^{-43} cm^3.

ENERGY SYSTEMATICS OF THE GIANT GAMOW–TELLER RESONANCE AND A CHARGE-EXCHANGE DIPOLE SPIN-FLIP RESONANCE

D.J. HOREN and C.D. GOODMAN[1]
Oak Ridge National Laboratory, Oak Ridge, TN 37830, USA

D.E. BAINUM
Emporia State University, Emporia, KS 66801, USA

C.C. FOSTER
Indiana University, Bloomington, IN 47401, USA

C. GAARDE
The Niels Bohr Institute, University of Copenhagen, Copenhagen, Denmark

C.A. GOULDING and M.B. GREENFIELD
Florida A&M University, Tallahassee, FL 32307, USA

J. RAPAPORT and T.N. TADDEUCCI
Ohio University, Athens, OH 45701, USA

E. SUGARBAKER and T. MASTERSON
University of Colorado, Boulder, CO 80302, USA

S.M. AUSTIN, A. GALONSKY and W. STERRENBURG
Michigan State University, East Lansing, MI 48824, USA

Received 21 October 1980

Energy systematics of the giant Gamow–Teller resonance and a charge-exchange resonance excited by a $L = 1, S = 1$ interaction are presented. Plots of the energy separation between each resonance and the IAS versus $(N - Z)/A$ can be represented approximately by linear functions.

In a series of papers [1–5] in the early 1960's, Fujita, Ikeda and Fujii explored the description of isobaric analogue states (IAS) in terms of proton particle–neutron hole pairs ($p\bar{n}$) and subsequently hypothesized the existence of a collective giant Gamow–Teller (GT) resonance to explain the hindrance of GT transitions in beta decay. In the absence of spin–orbit splitting, the energy separation between the GT and IAS was predicted [2–4] to be approximately linear with $(N-Z)/A$. These workers [2–4] also pointed out the probable existence of additional collective resonances of the type $\Delta l > 0$ and $\Delta S = 1$. Bohr and Mottelson [6] have discussed the general features of collective modes of excitation involving spin degrees of freedom. The first experimental observation of a giant GT resonance for $N > Z$ nuclei was reported by Doering et al. [7] from

[1] Now at Indiana University.

LOW-LYING ISOSCALAR DIPOLE EXCITATIONS IN ^{208}Pb

P. DECOWSKI
Institute of Experimental Physics, University of Warsaw, Poland

H.P. MORSCH
Institut für Kernphysik, Kernforschungsanlage Jülich, Jülich, West Germany

and

W. BENENSON
Cyclotron Laboratory, Michigan State University, East Lansing, USA

Received 16 February 1981

Inelastic excitations have been studied in 48 MeV α-scattering from ^{208}Pb. A concentration of isoscalar $L = 1$ strength is observed at $E_x \approx 5.5$ MeV which is interpreted as a dipole excitation mode representing a dipole oscillation of the nuclear diffuseness. A consistent description of inelastic excitations and electromagnetic widths is obtained.

During the last few years there has been growing interest in compressional modes of nuclear excitation, the simplest being the isoscalar monopole excitation. Low-lying monopole excitations [1,2] and particularly the high-frequency giant monopole resonance [3] has been subject of recent investigations. There is another simple compressional mode of excitation which so far has not been discussed very much, the isoscalar dipole excitation [4–6]. Recently, first experimental evidence has been obtained for a high-lying isoscalar dipole mode in ^{208}Pb [7]. In the present letter we discuss the concentration of isoscalar dipole strength in the low excitation region of ^{208}Pb ($E_x \approx 5.5$ MeV). This is interpreted in a collective model as a dipole oscillation of the nuclear diffuseness.

Experiments of inelastic α-scattering have been performed using a 48 MeV α-beam from the Michigan State University cyclotron. Targets of $\approx$1 mg/cm^2 enriched to 99.1% were deposited in vacuum on a 20 μg/cm^2 ^{12}C foil. Scattered particles were detected in a position-sensitive and particle-discriminating counter consisting of a delay-line wire counter attached to proportional and scintillation counters [8]. The counters were placed in the focal plane of an Enge split-pole magnetic spectrograph. The energy resolution (fwhm) was 35 keV. A spectrum taken at 23.5° is shown in fig. 1. The low-lying 1^- states [9], in particular the state at 5.50 MeV, are strongly excited. Angular distributions for the 3^- excitation at 2.61 MeV and for the excitation of 1^- states at 4.84, 5.28, 5.50, and 6.26 MeV are given in fig. 2. The diffraction pattern for the 1^- excitations is quite different from that of the 3^- excitation as well as of positive parity excitations.

The experimental data were analysed using a microscopic DWBA approach. A nucleon–nucleon force of gaussian form with a range of 1.68 fm and a volume integral of 446 MeV fm^3 was used which was folded into the α-particle density and the transition density for the target excited. Details of these calculations for the 3^- excitation are given in ref. [10]. As the α-nucleon interaction is isospin independent only isoscalar components of 1^- states are excited. For the low-lying excitations in question we use a collective model assuming a diffuseness oscillation proposed by Satchler [11]. In this model the diffuseness vibration is introduced in analogy to the shape vibrations as

0 031–9163/81/0000–0000/$ 02.50

$^{48}Ca(d,n)^{49}Sc$ reaction at $E_d = 20$ MeV; proton single-particle states in ^{49}Sc

Y. Iwasaki,* A. Galonsky, and D. J. Weber†
Cyclotron Laboratory, Michigan State University, East Lansing, Michigan 48824
(Received 15 January 1980)

The $^{48}Ca(d,n)^{49}Sc$ reaction has been studied at $E_d = 20$ MeV. Angular distributions of differential cross sections have been obtained for 14 transitions to states in ^{49}Sc up to an excitation energy of 7.1 MeV. A distorted-wave Born-approximation analysis has been made of the experimental data. With respect to states corresponding to the same proton single-particle orbital, relative values of derived spectroscopic factors are generally in good agreement with those obtained from $(^3He,d)$ reaction data. There are remarkable differences between the results from the $^{48}Ca(d,n)^{49}Sc$ reaction and the $^{48}Ca(^3He,d)^{49}Sc$, however, regarding the dependence of the relative spectroscopic factors on proton single-particle orbitals.

[NUCLEAR REACTIONS $^{48}Ca(d,n)^{49}Sc$, $E = 20$ MeV, neutron time of flight, $\Delta E = 120$ keV. Measured differential cross sections, 7.5°–50° lab. DWBA analysis, derived spectroscopic factors.]

I. INTRODUCTION

The first step in a microscopic study of a finite many-body system such as the atomic nucleus is to investigate the single-particle excitation spectrum. Locations and properties of neutron single-particle states in nuclei have been studied by the (d,p) reaction. The (d,n) reaction is the isobaric mirror reaction to the (d,p) reaction and is similar to it in reaction mechanism, but the (d,n) reaction has not generally been used for the study of proton single-particle states because of the difficulty of neutron detection with high energy resolution. Instead, proton single-particle states have been studied with the $(^3He,d)$ reaction, while its isobaric mirror reaction (t,d) has not generally been used for the study of neutron single-particle states because of problems associated with accelerating particles out of a radioactive gas. Thus, there is a remarkable asymmetry between the situations regarding neutron single-particle states and proton ones. It seems neither possible nor necessary to remove this asymmetry completely. It is always desirable, however, to check the mechanism of a reaction that is extensively used for spectroscopy by comparing it with other reactions.

The experimental work reported in the present paper was undertaken to obtain (d,n) reaction data that could be used to check the spectroscopic information derived from the $(^3He,d)$ reaction. Discrepancies have been noted (see end of Sec. IV) in which the target was not a closed core and, hence, might easily be excited. It was expected that the spectroscopic factors derived from the (d,n) and $(^3He,d)$ reactions would agree with one another better for doubly magic, closed core target nuclei than for others. The $^{48}Ca(d,n)^{49}Sc$ reaction was chosen as the most favorable case from the point of view of experimental feasibility. The final nucleus ^{49}Sc has a series of well-separated proton single-particle states. The large positive Q value (7.394 MeV) removes the problem of the most prevalent contaminants, ^{12}C and ^{16}O.

II. EXPERIMENTAL PROCEDURE AND RESULTS

The experiment on the $^{48}Ca(d,n)^{49}Sc$ reaction was performed at an incident deuteron energy of 20 MeV using the neutron time-of-flight facility[1] of the MSU isochronous cyclotron. The length of the neutron flight path was 34 m. Every third beam burst out of the cyclotron was transported to the target to observe states in ^{49}Sc up to an excitation energy of about 7 MeV. Neutrons were detected by a large liquid scintillation detector and associated electronic circuits.[1] Neutron time-of-flight spectra were measured in the laboratory angular range of 7.5° through 50°. The time resolution, defined as the FWHM of the target gamma-ray peak, was 0.93 ns. The FWHM of neutron peaks was about 120 keV. Figure 1 shows a doubled time-of-flight spectrum. By sending one stop pulse to the time-of-flight electronics for every two beam bursts on target, the events for a given state have been distributed into two peaks which are separated by the beam repetition period. This known separation provides a time calibration built into the spectrum. A very good feature of the spectrum is the smallness of peaks corresponding to contaminant ^{12}C and ^{16}O. There

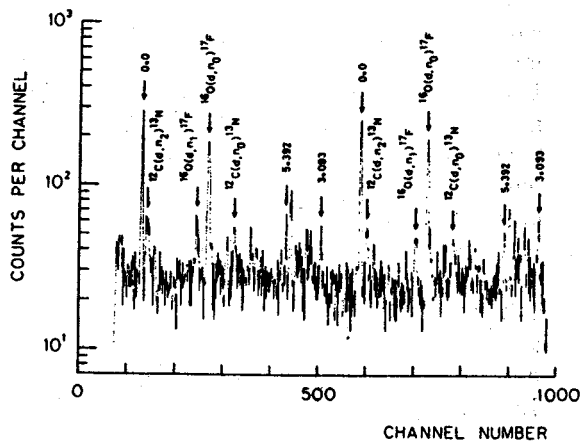

FIG. 1. Doubled neutron-time-of-flight spectrum measured at 25° lab. for the $^{48}Ca(d,n)^{49}Sc$ reaction with 20-MeV deuterons. Numerical values above arrows indicate excitation energies in ^{49}Sc in units of MeV. Peaks corresponding to contaminant ^{12}C and ^{16}O are also indicated. The time dispersion is 0.35 ns/channel. A representative energy dispersion, that at the 3.093-MeV state, is 34 keV/channel.

PHYSICAL REVIEW C VOLUME 22, NUMBER 2 AUGUST 1980

Electromagnetic multipole moments of ground states of stable odd-mass nuclei in the *sd* shell

B. A. Brown
Nuclear Physics Laboratory, Oxford University, Oxford OX1 3RH, England

W. Chung
Cyclotron Laboratory, Michigan State University, East Lansing, Michigan 48828

B. H. Wildenthal
Nuclear Physics Laboratory, Oxford University, Oxford OX1 3RH, England
and Cyclotron Laboratory, Michigan State University, East Lansing, Michigan 48824

(Received 23 January 1980)

Shell-model wave functions for $A = 17$–39 nuclei are used to calculate the one-body densities upon which are based the $M1$, $E2$, $M3$, $E4$, and $M5$ moments of stable ground states with $J^\pi = 3/2^+$ and $5/2^+$. Values of the moments are obtained by combining these densities with single-particle matrix elements calculated with both free space and renormalized expressions for the electromagnetic operators. These results extend previous calculations for the $M1$ and $E2$ moments. The theoretical values are analyzed in terms of deviations from the predictions of the pure-configuration shell model and compared with available experimental data. While several of these data are well described with the present theory, a few other experimental values differ significantly from the corresponding predicted values.

[NUCLEAR STRUCTURE ^{17}O, ^{21}Ne, ^{23}Na, ^{25}Mg, ^{27}Al, ^{33}S, ^{35}Cl, ^{37}Cl, ^{39}K; calculations for the $M1$, $E2$, $M3$, $E4$, and $M5$ moments of ground states; complete $0d_{5/2}$-$1s_{1/2}$-$0d_{3/2}$ shell-model wave functions; Chung-Wildenthal Hamiltonians.]

I. INTRODUCTION

Extensive data exist for the magnetic dipole and electric quadrupole moments of nuclear states. These data provide qualitative guides to the structure of the associated nuclear state, allow quantitative tests of theoretical wave functions via comparison of measured to predicted moment values, and ultimately, with accurate enough theoretical wave functions, can be analyzed to yield information about the effects of the finite nuclear medium upon the basic nucleonic operators. Measured values of the $M1$ and $E2$ moments of nuclei in the *sd* shell ($A = 17$–39) have been recently compared with the predictions of a comprehensive and mutually consistent set of wave functions calculated in the *sd*-shell-model space.[1-3] The results of these comparisons suggest that the significant effects of intra-*sd*-shell configuration mixing upon the observed moments can be accounted for accurately enough by the theoretical wave functions that meaningful information can be extracted about the renormalizations which are appropriate for this mass region and model space for the $M1$ and $E2$ operators.

In this paper we present predictions from these same model wave functions for $M3$, $E4$, and $M5$ moments. The possibilities for experimental measurements of these higher moments are much more restricted than for the dipole and quadrupole cases. The $M3$ moments of ^{35}Cl and ^{37}Cl have been measured by atomic beam techniques; the accuracy of these measurements are limited by theoretical uncertainties in the electronic wave functions. At present, elastic electron scattering seems to offer the best technique for measuring $M3$, $E4$, and $M5$ moments. We present here shell-model results for the ground states of stable *sd*-shell nuclei which have such higher moments, namely ground states with $J^\pi = \frac{3}{2}^+$ and $\frac{5}{2}^+$. Even though the higher moments form a less extensive field for study than do the conventional dipole and quadrupole cases, the added dimensions they bring to our perception of nuclear structure, particularly when all facets of the multipole structure can be incorporated into a unified theory, make experimental pursuit of this kind of information highly desirable.

The present paper is organized in an attempt to make clear the different components of theoretical predictions of moment values and their relative importance. We first note the formal relationship by which the shell-model one-body densities and the single-particle matrix elements of the electric and magnetic operators are combined to yield values of the moments. The roles of the single-particle radial wave functions and of operator renormalization in the evaluation of the single-parti-

PHYSICAL REVIEW C VOLUME 22, NUMBER 2 AUGUST 1980

Effective $M3$ operator and relevant transitions in ^{24}Al, ^{24}Na, ^{34}Cl, ^{38}K, and ^{38}Cl

B. A. Brown and S. E. Massen*
Nuclear Physics Laboratory, Oxford University, Oxford OX1 3RH, England

W. Chung
Cyclotron Laboratory, Michigan State University, East Lansing, Michigan 48824

B. H. Wildenthal
Nuclear Physics Laboratory, Oxford University, Oxford OX1 3RH, England
and Cyclotron Laboratory, Michigan State University, East Lansing, Michigan 48824

T. A. Shibata
Department of Physics, University of Tokyo, Bunkyo-ku, Tokyo, Japan
(Received 7 February 1980)

Theoretical calculations are presented for the magnetic octupole electromagnetic matrix elements in light nuclei. Shell-model wave functions are used to calculate the $M3$ matrix elements for the cases ^{24}Al $1^+ \rightarrow 4^+$, ^{24}Na $1^+ \rightarrow 4^+$, ^{34}Cl $3^+ \rightarrow 0^+$, ^{38}K $0^+ \rightarrow 3^+$, and ^{38}Cl $5^- \rightarrow 2^-$. The radial matrix elements are calculated with harmonic-oscillator and spherical Hartree-Fock potentials. The comparison of the calculated and experimental matrix elements is expressed in terms of effective spin g factors. Theoretical calculations for the core-polarization corrections are presented and relations between the $E2$ core-polarization charge and the $M3$ effective spin g factors are derived.

[NUCLEAR STRUCTURE ^{24}Na, ^{24}Al, ^{34}Cl, ^{38}K, ^{38}Cl; calculations of $M3$ decay strengths; extraction of effective $M3$ operator; full $d_{5/2}$-$s_{1/2}$-$d_{3/2}$ shell-model calculations with Chung-Wildenthal Hamiltonians.]

I. INTRODUCTION

Recent electron scattering experiments have obtained interesting new information about the high ($L \geq 3$) multipole moments of nuclei.[1-3] Previously, nuclear models have been predominantly tested by and designed to explain $E0$, $E1$, $E2$, and $M1$ matrix elements. The higher moments will provide new and hopefully discriminating tests of the predictions of these models. The $M1$ matrix elements for $A = 17$–39 nuclei are quite well accounted for by shell-model calculations within a full $(sd)^n$ basis using g factors very close to the free-nucleon values.[4] The large $E2$ matrix elements in this region are also well accounted for by these same shell-model calculations if a constant isoscalar enhancement factor of $1 + \delta e_p + \delta e_n = 1.7 \pm 0.1$ is used.[5] This enhancement can be understood as a core-polarization effect involving the rearrangement of particles in the orbits below and above the sd orbits.

In the context of these results for $M1$ and $E2$ phenomena, it was initially surprising that the $M3$ matrix element observed in the electron scattering from ^{17}O (Ref. 1) was much smaller than the value predicted for a $d_{5/2}$ neutron single particle. However, subsequent calculations[6-8] have shown that a hindrance of the $M3$ matrix elements can be understood by the same core-polarization mechanism that gives rise to the enhancement of the $E2$ matrix elements.

Unfortunately, it is difficult to extract a precise value for the $M3$ matrix element in ^{17}O because the magnetic electron scattering cross section is dominated by the $M1$ and $M5$ contributions.[1] The situation is similar for the elastic electron scattering on other nuclei with $\frac{5}{2}^+$ ground states.[2,3] In the next few years much more information on the $M3$ matrix element will become available from elastic electron scattering on the nuclei with $\frac{3}{2}^+$ ground states, as well as inelastic excitation of 3^+ states in even-even nuclei, but at present the only other source of information on this topic comes from the few precisely measured half-lives of $M3$ gamma decays in the sd shell. It is the purpose of the present work to concentrate on the shell-model predictions for these $M3$ gamma decays.

In the sd shell nuclei only three $M3$ gamma decay half-lives have been measured: in ^{24}Al, ^{24}Na, and ^{34}Cl. The experimental properties are given in Table I. Presented in addition in Table I is information on ^{38}Cl which will be discussed briefly in Sec. V in terms of a $d_{3/2}f_{7/2}$ configuration. The experimental situation for ^{24}Al has been much improved by recent experiments[9,10] which have shown that the previous assignment[11] of a 439 keV gamma ray in ^{24}Al was in error.

The configuration mixing among the $d_{5/2}s_{1/2}$ and $d_{3/2}$ orbits is large for the $A = 24$ and $A = 34$ nuclei,

Compressibility and the monopole collective field

F. Serr and G. Bertsch
Cyclotron Laboratory and Physics Department, Michigan State University, East Lansing, Michigan 48824

J. P. Blaizot
Service de Physique Theorique, CEN Saclay, B.P. No. 2, 91190 Gif-sur-Yvette, France

(Received 26 December 1979)

We show the relation between conventional random phase approximation and the collective field description of monopole vibrations by Hamamoto and Mottelson. When surface compression is properly included, the collective treatment yields the same vibrational frequency as conventional random phase approximation, for a given compressibility.

[NUCLEAR STRUCTURE Giant monopole vibrations, surface effects, relation to compressibility.]

The compressibility of nuclear matter is an important parameter which, unlike the binding energy and saturation density, cannot be obtained directly from static properties of finite nuclei. The giant monopole resonance is currently the main source of empirical information on the compressibility. There has been, however, some controversy over the value of the bulk compressibility K, implied by the monopole frequency. Blaizot *et al.*[1] have performed self-consistent calculations of the giant monopole resonance in spherical nuclei in the random phase approximation (RPA). This analysis[2] indicates that a compressibility $K = 210 \pm 30$ MeV successfully reproduces the data. However, Hamamoto and Mottelson[3] found that a macroscopic model of collective fields for the monopole vibration in ^{208}Pb required that $K = 400$ MeV.

One suggested explanation for this discrepancy was a difference in effective mass m^*, used in the two calculations. This is not the case. We present below RPA calculations with Skyrme-type interactions having $m^*/m = 1$ which are consistent with the analysis of Ref. 2. The origin of the discrepancy is instead in the functional form assumed for the surface field in the macroscopic model. It is necessary to include the effect of compression in the surface field. We show this by tracing the connection between the models, and examining the effect on the energy of different assumptions for the surface field.

Our microscopic calculations employ the response function formalism with coordinate-space Green's functions.[4] We sketch here the important points. The particle-hole Green's function, $G(r, r', \omega)$, is given in the RPA by

$$G^{\mathrm{RPA}} = G^0\left(1 - \frac{\delta V}{\delta \rho} G^0\right)^{-1}, \tag{1}$$

where the bare Green's function, G^0, may be written as

$$G^0(r, r', \omega) = \sum_{p,h} \phi_p^0(r)\phi_h^0(r)\left[\frac{1}{\omega - (\epsilon_p - \epsilon_h)} - \frac{1}{\omega + (\epsilon_p - \epsilon_h)}\right] \times \phi_p^0(r')\phi_h^0(r'). \tag{2}$$

The poles of G identify the natural resonances of the system. The density perturbation induced by an external field of the form $V_{\mathrm{ext}}(r)\exp(-i\omega t)$ is given by

$$\delta\rho(r) = \int G^{\mathrm{RPA}}(r, r', \omega) V_{\mathrm{ext}}(r') d^3r'. \tag{3}$$

If V_{ext} excites a single eigenstate ψ_n, as it would near a resonance, this is proportional to the transition density $\delta\rho = \langle n | \hat{\rho} | 0 \rangle$. Equations (1)–(3) are solved as matrix equations on a coordinate space mesh.

The calculations start with the Hartree-Fock ground state of ^{208}Pb. We use a velocity-independent Skyrme interaction,[5] with parameters $t_0 = -1100$ MeV fm^3, $t_3 = 16\,000$ MeV fm^6, $t_1 = t_2 = x = 0$. The absence of momentum dependence implies that $m^*/m = 1$. At saturation density $\rho_0 = 0.16$ fm^{-3}, the compressibility $K = 418$ MeV, with contributions of 221 MeV from the kinetic energy and 197 MeV from the potential. This particular interaction gives $\langle r^2 \rangle^{1/2} = 5.3$ fm for ^{208}Pb and a single-particle spectrum which is somewhat overbound, but is adequate for the purposes of our

PHYSICAL REVIEW C VOLUME 22, NUMBER 3 SEPTEMBER 1980

Effective S-wave πNN interaction in nuclei

D. O. Riska and H. Sarafian
Department of Physics, Michigan State University, East Lansing, Michigan 48824
(Received 21 February 1980)

We show that virtual pion rescattering in a nuclear medium gives rise to an effective S-wave πNN interaction Hamiltonian. The first few terms in the density expansion of the strength parameter are estimated and shown to be appreciable in nuclear matter.

[NUCLEAR REACTIONS Pion-nucleus interactions: S-wave interaction.]

Considerable, if inconclusive, attention has been given in recent literature to the "Barnhill" ambiguity in the S-wave πNN interaction in nuclei.[1-5] The ambiguity concerns the strength parameter λ in the Hamiltonian for this interaction:

$$H = \lambda \frac{f}{\mu} \psi^{\dagger} \vec{\sigma} \cdot \vec{\nabla}_N \vec{\tau} \cdot \vec{\phi} \psi . \tag{1}$$

Here ψ and $\vec{\phi}$ are the nucleon and isovector pion field operators and $\vec{\nabla}_N$ a symmetrized gradient operator acting on the nucleon fields.[1] In (1) f is the pseudovector pion-nucleon coupling constant ($f^2/4\pi = 0.08$) and μ the pion mass.

Straightforward nonrelativistic reduction of the Lorentz invariant pseudovector πNN interaction Hamiltonian leads to $\lambda = \mu/2m$ (m = nucleon mass). The unitary freedom inherent in this reduction leads to the ambiguity in λ.[1] The physical reason for this ambiguity is the lack of a definite treatment of the binding effects in a nuclear medium that force the nucleon under consideration off shell.[3,4] Only in simplified boson exchange models is it possible to make definite predictions for λ.[6] Therefore it has been suggested that the parameter be determined empirically by means of (p,π^+) and (π^+,p) reactions interpreted with a single nucleon stripping model.[3,7] Apart from the obvious criticism that the simple stripping model may not be adequate, we shall in this work show that sizeable density dependent medium corrections to the effective one-body operator (1) are caused by virtual pion rescattering. Thus λ will not have any universal value valid for a range of nuclei, and attempts at empirical determination of λ will be futile.

The main rescattering process that contributes to λ is that involving two nucleons: an incident S-wave pion rescatters off a nucleon (which is ejected) and is absorbed by a particle-hole pair, or it rescatters off a particle-hole pair and is absorbed by a final nucleon (which is ejected). This is illustrated in the diagrams in Fig. 1, which include direct and exchange terms. These processes take place in addition to "true" two-nucleon absorption processes in which two nucleons are ejected from the nucleus.

The diagram in Fig. 1(c) represents distortion of the incident pion wave function and should not be included in the basic πNN interaction, as the distortion can be treated with an optical potential. The corresponding exchange term in Fig. 1(d) should be excluded for the same reason. The amplitude for the diagram in Fig. 2(a) vanishes in spin or isospin 0 nuclei because of the spin-vector isovector nature of the πNN absorption operator. Therefore only the remaining exchange term diagram [Fig. 1(b)] contributes to the S-wave absorption interaction.

In order to construct the amplitude corresponding to Fig. 1(b) we employ the phenomenological zero-range Hamiltonian

$$H = 4\pi \frac{\lambda_1}{\mu} \vec{\psi}\vec{\phi} \cdot \vec{\phi}\psi + 4\pi \frac{\lambda_2}{\mu^2} \vec{\psi}\vec{\tau} \cdot \vec{\phi} \times \vec{\pi}\psi \tag{2}$$

to describe the S-wave rescattering vertex ($\vec{\pi} = \partial_0 \vec{\phi}$). In (2) the coupling constants λ are de-

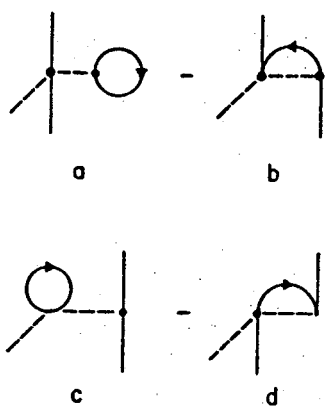

FIG. 1. Pion rescattering contributions to the effective S-wave πNN interaction.

PHYSICAL REVIEW C VOLUME 22, NUMBER 4 OCTOBER 1980

Elastic scattering of ^{6}Li at 73.7 MeV

R. Huffman,* A. Galonsky, R. Markham,† and C. Williamson‡
Cyclotron Laboratory, Michigan State University, East Lansing, Michigan 48824
(Received 6 December 1979)

Angular distributions for ^{6}Li elastic scattering at 73.7 MeV from targets of ^{58}Ni, ^{90}Zr, ^{124}Sn, and ^{208}Pb have been measured. Optical-model parameters for Woods-Saxon real and imaginary volume potentials have been found which describe the data well and exhibit both discrete and continuous ambiguities. For a fixed geometry, the dependence of the optical potentials on Z and A of the target and on the bombarding energy was investigated.

[NUCLEAR REACTIONS ^{58}Ni, ^{90}Zr, ^{124}Sn, ^{208}Pb (^{6}Li, ^{6}Li), E = 73.7 MeV; measured $\sigma(\theta)$; deduced optical-model parameters.]

I. INTRODUCTION

There have been studies of ^{6}Li elastic scattering by medium- and heavy-weight nuclei with bombarding energies between 30 and 50 MeV (Refs. 1-5) and above 100 MeV.[6] The motivation for this study was to provide optical-model parameters at an intermediate energy, namely 73.7 MeV. The parameters are presented for use in direct-reaction calculations and, when coupled with the results at higher and lower bombarding energies, may be used to investigate the systematics of ^{6}Li elastic scattering. The present study uses targets of ^{58}Ni, ^{90}Zr, ^{124}Sn, and ^{208}Pb. The dependence of the potential depths on the Z and A of the target and on the bombarding energy has been investigated.

II. EXPERIMENTAL PROCEDURE

A beam of 73.7 MeV ^{6}Li^{+++} ions was produced by the MSU sector-focused cyclotron. The beam was produced by an arc-type ion source[7] which employed the sputtering action of Ne on ^{6}Li enriched LiF pellets. The beam was transported to a 1-m scattering chamber where elastic-scattering measurements were taken. The transport system, consisting of two analyzing magnets and several quadrupole focusing magnets, produced a beam spot approximately 2 mm by 4 mm as viewed with an MgO scintillator. On-target beam currents of 1-100 nA were monitored by stopping the beam in a Faraday cup. An Ortec charge digitizer was employed to integrate the beam current from the Faraday cup in order to obtain charge measurements for each experimental point.

The targets employed in this study were isotopically enriched, self-supporting foils with average thicknesses as follows: ^{58}Ni, 3.8 mg/cm^2; ^{90}Zr, 10.2 mg/cm^2; ^{124}Sn, 5.1 mg/cm^2; ^{208}Pb, 10.3 mg/cm^2. The average thicknesses were obtained by weighing the targets with a precision balance and by measuring the surface area. An alpha-particle gauge was then used to investigate the central region of each target in order to determine thickness uniformity in the beam-spot region. The alpha-gauge measurements revealed relative variations of ±3% for the Ni, Zr, and Sn targets and ±12% for the Pb target.

Detection of the scattered ^{6}Li^{+++} ions was made by using two ΔE-E telescopes mounted symmetrically on opposite sides of the beam axis. The detectors in both telescopes were Ortec silicon surface barrier detectors with thicknesses of ~ 100 μm for the ΔE detector and ~1000 μm for the E detector. The angular acceptance of each telescope was defined by a collimator placed at the front of the telescope. For each telescope, the angular acceptance was 0.3° for angles less than 30° and 1° for angles greater than 30°. The detector arrangement provided two advantages over a single-telescope-plus-fixed-monitor arrangement. Continuous monitoring of any beam drift from the true beam axis was provided by comparison of the yields in the elastic peaks of the two telescopes after each measurement. For a slight misalignment, $\Delta\theta$, the average value of the two yields is correct to second order, since one angle is $\theta + \Delta\theta$ and the other is $\theta - \Delta\theta$. A difference between yields indicated that the beam had moved slightly from the original beam axis, and a realignment of the beam could be made before the next measurement. The other advantage was that the use of a second telescope produced an improvement in statistical accuracy by a factor of $\sqrt{2}$. Due to the low beam currents, the angular range of measurements was limited by a combination of time and decreasing cross section with angle.

The pulses from both telescopes were processed by the same octal ADC and were, thus, subject to the same system dead time. Two measurements for the dead time were made simultaneously using pulses from the charge digitizer and from the ADC strobe. Each set of pulses was counted by two scalers, one of which was inhibited whenever the ADC was busy. The ratio was the fractional live time. The two determinations were always within one percent of each other. A two-dimensional ΔE vs (E + ΔE) display was used for each telescope for particle identification and for gating of the spectrum of interest. The elastic peaks in the gated spectra had resolutions of ~ 400 keV (FWHM). Spectra were taken in one-degree steps from 8° to 30° and in two-degree steps for angles greater than 30°. The maximum angle measured (in the lab) was 50° for Ni, Zr, and Pb and 56° for Sn. Points taken at the start of a run were repeated at the end; agreement was always within statistics.

III. EXPERIMENTAL RESULTS

The measured ^{6}Li angular distributions are shown in Fig. 1. The indicated errors are relative errors only. Where there is no error indicated, the error is smaller then the point size. At large angles, the errors are primarily statistical due to low counting rates. At all angles there are small cross-sectional errors due to uncertainties in the settings and readouts of the angular positions of the detectors. These differ from angle to angle, since they are a function of the slope of the angular distribution. There are also small uncertainties due to possible beam drifts across the somewhat nonuniform central region of each target. The relative errors are generally $\leq \pm 4\%$ for all but the largest angles. The absolute errors

PHYSICAL REVIEW C VOLUME 22, NUMBER 4 OCTOBER 1980

Test of the isobaric multiplet mass equation from β-delayed proton decay of ^{24}Si

A. G. Ledebuhr, L. H. Harwood, and R. G. H. Robertson
Cyclotron Laboratory and Department of Physics, Michigan State University, East Lansing, Michigan 48824

T. J. Bowles*
Physics Division, Argonne National Laboratory, Argonne, Illinois 60439
(Received 21 January 1980)

The highly proton-rich nucleus ^{24}Si has been produced via the ^{24}Mg(^{3}He,3n) reaction. The half-life of ^{24}Si was found to be 103(42) ms, and the energy of the protons de-exciting the $T = 2$ state in the daughter, ^{24}Al, has been measured as 3912.7(37) keV. From detailed consideration of masses in the $A = 24$ isobaric quintet (recently completed), it is concluded that this quintet constitutes a test of the isobaric multiplet mass equation as precise as the mass 9 quartet and that there is, in this case, no significant departure from the equation.

[RADIOACTIVITY ^{24}Si; from ^{24}Mg(^{3}He, 3n); measured $T_{1/2}$, E_p (β-delayed protons).]

I. INTRODUCTION

The isobaric multiplet mass equation (IMME) is a result of first order perturbation theory, with the assumption that only two-body forces are responsible for charge-dependent effects in nuclei. The equation predicts that the mass excesses ΔM of analog states of an isobaric multiplet can be determined by a three-parameter quadratic equation

$$\Delta M = a + bT_z + cT_z^2 .$$

Deviations from the quadratic form of the IMME could be expected if there were charge dependent many-body nuclear forces, isospin mixing, or shifts in unbound levels. These deviations are usually parametrized as cubic and quartic terms in T_z (dT_z^3, eT_z^4). If an isobaric quintet ($T = 2$ multiplet) is used to test this equation, both additional terms can be determined, whereas only one can be determined in a quartet ($T = \frac{3}{2}$ multiplet).

There are now 22 complete isobaric quartets, and in one case, the ground state $A = 9$ quartet, a significantly nonzero d coefficient, 5.8(16) keV, is found.[1] However, mass 9 is also the most accurately measured multiplet and one cannot conclude that this deviation is exceptional without obtaining results of comparable accuracy in other multiplets. Isobaric quintets offer the prospect of improved tests of the IMME. This paper describes measurements which yield a test of the IMME in the $A = 24$ quintet of the same level of precision as the mass 9 quartet. There are now four completed isospin quintets, the $A = 8$, 20, 24, and 36 multiplets.[1-7] The $A = 8$ quintet shows a slight deviation from the IMME.

In the $A = 24$ quintet, the mass of the $T_z = 2$ nucleus ^{24}Ne was measured by Silbert and Jarmie[8] using the ^{22}Ne(t,p)^{24}Ne reaction. The most accurate measurement of the lowest $T = 2$ state in ^{24}Na was made by Start *et al.*[9] via the ^{22}Ne(^{3}He,$p\gamma$) reaction, and earlier work has been summarized by Endt and van der Leun.[10] The lowest $T = 2$ level in ^{24}Mg was first observed in the ^{26}Mg(p,t) reaction by Garvey, Cerny, and Pehl.[24] It has subsequently been studied as an isospin-forbidden resonance in the ^{23}Na(p,γ) reaction by Riess *et al.*,[11] by Szücs, Underwood, Alexander, and Anyas-Weiss,[12] and by Heggie and Bolotin.[13]

The $T = 2$ level in ^{24}Al, which is the subject of this paper, has recently been discovered at the Lawrence Berkeley Laboratory. In the experiments of Äystö *et al.*,[4] the reaction ^{24}Mg(^{3}He, 3n) was used to produce the parent beta activity ^{24}Si, which was transported using a helium jet to an on-line mass separator system. Mass-24 activity was deposited in front of a ΔE-E telescope. Measurement of the energy of protons emitted in the decay of the $T = 2$ state of ^{24}Al (populated by the β-decay of ^{24}Si) gave a result for the mass of the state accurate to 9 keV.

The quintet has been completed with the observation of ^{24}Si in the ^{28}Si(^{4}He, ^{8}He) reaction by Tribble *et al.*[5] The mass of ^{24}Si was determined to an accuracy of 22 keV.

In a previous paper,[14] the description of a cryogenic (liquid-nitrogen cooled) helium jet coupled to a recoil time-of-flight mass analyzer for use in observing short-lived β-delayed particle emitters was presented. This apparatus was used at Princeton University in an attempt to observe ^{24}Si. Results tentatively suggested that protons from the decay of this nucleus had been observed and that the mass of the $T = 2$ state in the daughter nucleus ^{24}Al was consistent with the prediction from the quadratic form of the IMME. With these promising

PHYSICAL REVIEW C VOLUME 22, NUMBER 5 NOVEMBER 1980

Correlated fission fragments emitted in the reaction of ^{16}O on ^{238}U at 20 MeV/nucleon

B. B. Back, K. L. Wolf, and A. C. Mignerey*
Chemistry Division, Argonne National Laboratory, Argonne, Illinois 60439

C. K. Gelbke and T. C. Awes
Cyclotron Laboratory, Michigan State University, East Lansing, Michigan 48824
and Lawrence Berkeley Laboratory, University of California, Berkeley, California 94720

H. Breuer and V. E. Viola, Jr.
Department of Chemistry, University of Maryland, College Park, Maryland 20742

P. Dyer
Cyclotron Laboratory, Michigan State University, East Lansing, Michigan 48824
(Received 21 April 1980)

The reactions induced by 315-MeV ^{16}O ions on ^{238}U have been studied by observing the folding angle between the two fission fragments resulting from the sequential fission decay of the target residue in coincidence with reaction products ranging from protons to ^{16}O ions. A kinematical analysis shows that the emission of light particles (p,d,t,α) plays an important role for both central and peripheral reactions. It is concluded that these particles, most likely, are emitted during the early stages of the reaction.

[NUCLEAR REACTIONS, FISSION $^{238}U(^{16}O,Xf)$, $X=p,d,t,\ldots,O$, $E=315$ MeV; measured $\sigma(E_x)$ and fission fragment folding angle distributions. Deduced missing momentum and fission fragment mass distributions.]

I. INTRODUCTION

Heavy ion reactions at bombarding energies below 10 MeV/nucleon have been studied intensively during recent years and the basic reaction mechanism is currently known in some detail.[1-4] The main contributions to the reaction cross section are compound nucleus formation and deep inelastic processes, both of which lead to subsequent particle decay, γ emission, or fission. Light particle spectra observed in these reactions can, to a remarkable degree, be accounted for by evaporation from thermally equilibrated, fully accelerated reaction partners or fission fragments.[5-7] However, there is evidence of some pre-equilibrium particle emission, mostly in connection with compound nucleus formation processes.[8-11] These effects are significantly more important, for both central and peripheral collisions, when the bombarding energy is increased to 20 MeV/nucleon.

In the present experiment we have studied the reactions resulting from the bombardment of a ^{238}U target with ^{16}O ions. We have chosen to investigate reactions on an actinide target (^{238}U) because of its low fission threshold.[12] As a consequence, fission is the dominant decay mode of the target residue and little selectivity is imposed on the reaction by requiring a fission coincidence. (Of course, a minimum inelasticity has to be required for the reaction to produce two fission fragments.) Detecting fission fragments in coincidence with other outgoing reaction products, therefore, imposes only a small bias on the reaction investigated and allows the study of rather global features of the reaction. Furthermore, by studying the fission decay in more detail we obtain information on the excitation energy of the target residues after the reaction has taken place. Thus, the folding angle between the resulting fission fragments is closely related to the amount of linear momentum transferred to the fissioning system[13,14] and the fission fragment mass distribution is, to some degree, a measure of the excitation energy of the fissioning nucleus. In this paper we will give a detailed description of the experimental setup and analysis, and discuss the results in terms of various models applicable to this energy regime. Some aspects of the present work have been published earlier in brief reports.[15,16]

II. EXPERIMENTAL ARRANGEMENT

Beams of 140 and 315 MeV ^{16}O ions were provided by the 88" cyclotron at the Lawrence Berkeley Laboratory. The target consisted of 200 $\mu g/cm^2$ $^{238}UF_4$ material evaporated onto a 50 $\mu g/cm^2$ carbon foil. The detector arrangement is illustrated in Fig. 1. Two position sensitive solid state detectors (PSD) were placed on opposite sides of the beam axis, which allows for the simultaneous measurement of both fission fragment energies and laboratory angles. These detectors

PHYSICAL REVIEW C VOLUME 22, NUMBER 5 NOVEMBER 1980

Collapse of the conventional shell-model ordering in the very-neutron-rich isotopes of Na and Mg

B. H. Wildenthal*
Los Alamos Scientific Laboratory, Los Alamos, New Mexico 87544

W. Chung
Cyclotron Laboratory, Michigan State University, East Lansing, Michigan 48824
(Received 31 March 1980)

Recent experimental data on the structure of the very-neutron-rich isotopes of Na and Mg show sharp departures at $N = 20$ from the predictions of conventional $d_{5/2}$-$s_{1/2}$-$d_{3/2}$ shell-model calculations.

[NUCLEAR STRUCTURE Isotopes of Na and Mg; calculated ground state energies, magnetic dipole moments, and excitations of 2^+ states; $0d_{5/2}$-$1s_{1/2}$-$0d_{3/2}$ shell model, Chung-Wildenthal Hamiltonians.]

It has often been speculated that study of far-from-stability nuclei would reveal exciting and instructive extensions to our knowledge of nuclear structure as it has been accumulated from the study of systems with stable or near-stable neutron/proton ratios. Results emerging from an ongoing research program on the neutron-rich Na isotopes and their decay products[1-3] seem to fulfill such expectations. The first data to emerge from this program were the masses of the Na isotopes up through ^{32}Na.[1] The values which were obtained for ^{30}Na and ^{31}Na indicated significantly more binding energy for these systems than was predicted by conventional shell-model calculations[4] based on the then most firmly based effective interaction.[5] Subsequent Hartree-Fock calculations[6] suggested that these mass anomalies, together with the large binding energy of ^{32}Na, are associated with a shape transition which results in the filling, at large prolate deformations, of the negative-parity $f_{7/2}$ orbit in preference to the $d_{3/2}$ orbit.

Additional experimental information about these systems—the ground-state spins and magnetic moments of the Na isotopes[2] and the energies of the first excited states of some Mg isotopes[3]—has recently become available. We examine here the amalgam of these data in comparison to newer, more extensive shell-model calculations.[7] Our aim is to delineate in detail the degree to which these experimental data on "exotic" nuclei contradict conventional nuclear-structure expectations.

We utilize two complementary sets of shell-model results. Each set systematically utilizes the complete $d_{5/3}$-$s_{1/2}$-$d_{3/2}$ basis space and is founded upon the assumption that $0p$ and $0f1p$ degrees of freedom can be neglected in the description of lowest-lying states in the region $8 \leq N$, $Z \leq 20$. One set of results is based on an effective interaction (the "particle" Hamiltonian) determined by a fit to 200 level energies taken predominantly from the $A = 18$–24 mass region. The other is based on an interaction (the "hole" Hamiltonian) analogously determined from a fit to level energies taken predominantly from the $A = 32$–38 region. The predictions of these calculations explain a wide variety of structural features in the $A = 18$–26 and $A = 30$–38 regions rather accurately and have been used in the $A = 28$ region with fair success. Neither calculation is tailored to deal with the exotic Na and Mg isotopes, but inspection of how the agreement between these calculations and experimental data extrapolates away from the regions in which the effective interactions were determined suggests that their predictions should explain the qualitative aspects of the observed structure as long as the dominant degrees of freedom are those of the *sd* shell.

We consider first the experimentally assigned ground-state spins of the Na isotopes. Since shell-model calculations yield a definite energy-ordered sequence of nuclear spins, it is implicit that the spin of the observed ground state should correspond to that of the calculated ground state. In the case of close-lying ground-state multiplets, however, it is not critical if the theoretical and experimental spin orderings are not identical so long as the appropriate identifications are made. Up through ^{30}Na, the calculated and measured[2,8,9] ground-state spins (^{20}Na-2^+, ^{21}Na-$\frac{3}{2}^+$, ^{22}Na-3^+, ^{23}Na-$\frac{3}{2}^+$, ^{24}Na-4^+, ^{25}Na-$\frac{5}{2}^+$, ^{26}Na-3^+, ^{27}Na-$\frac{5}{2}^+$, ^{28}Na-1^+, ^{29}Na-$\frac{3}{2}^+$, ^{30}Na-2^+) are in agreement, even though the energy differences between the $J^\pi = \frac{5}{2}^+$ and $\frac{3}{2}^+$ states in the odd isotopes are small and the odd-neutron, odd-proton even-mass isotopes have

Projected Hartree-Fock calculations for ^{52,53}V

Surender Saini*
Nuclear Physics Division, Bhabha Atomic Research Centre, Bombay - 400 085, India
and Cyclotron Laboratory, Michigan State University, East Lansing, Michigan 48824

M. R. Gunye
Theoretical Reactor Physics Section, Bhabha Atomic Research Centre, Bombay - 400 085, India
(Received 20 June 1980)

The structure of the low-lying nuclear states in neutron rich isotopes of vanadium ^{52,53}V is investigated. The investigations are carried out in the framework of Hartree-Fock projection formalism by employing a realistic nucleon-nucleon interaction. All the valence nucleons outside the inert ^{40}Ca core are considered to be active in the configuration space of the full *fp* shell. The energy levels, static electromagnetic moments, and the electromagnetic transition probabilities are evaluated from the band-mixing calculations, wherein the lowest few energetically close intrinsic states of the nuclei are taken into account. The results of the present calculations are in fair agreement with the available experimental data.

[NUCLEAR STRUCTURE Vanadium isotopes: calculated energy levels, static moments, $B(E2)$ and $B(M1)$. Hartree-Fock projection formalism, realistic nucleon-nucleon interaction, band mixing.]

I. INTRODUCTION

Properties of the nuclei in the *fp*-shell region are currently of considerable experimental and theoretical interest. In recent years a large amount of experimental data, especially on high spin states, has become available through the study of heavy-ion induced fusion-evaporation type of reactions. Shell model calculations for the $20 \leq Z \leq 28$ and $N = 29$ isotones have been previously reported by Vervier[1,2] and by Horie and Ogawa,[3] and for the $N = 30$ isotones by Vervier,[2] McGrory,[4] and Horie and Ogawa.[5] None of these calculations, however, investigate the high spin states in the nuclei under consideration. Recently Nathan *et al.*[6] have reported the results of their shell model calculations on the yrast spectra of many nuclei in the range $20 < Z < 28$ and $28 < N < 40$. In all these calculations, an inert ^{48}Ca core was assumed, and the active protons were confined to the $0f_{7/2}$ orbital and the active neutrons to the $0f_{5/2}$, $1p_{3/2}$, and $1p_{1/2}$ orbitals, i.e., to the configuration space $(\pi 0f_{7/2})^n \times (\nu 1p_{3/2}, 0f_{5/2}, 1p_{1/2})^m$, where $n = Z - 20$ and $m = N - 28$. Moreover, all the shell model calculations mentioned above employ empirical nucleon-nucleon interactions. In the Horie and Ogawa[5] calculations for ^{53}V, the first six eigenstates are predominantly due to recoupling members of the $(f_{7/2})^3$ configuration. In that case, the dipole transitions between these states would be strictly forbidden. The observation[7] of $M1$ transitions between these states, however, indicates the presence of other admixtures, e.g., those resulting from the promotion of protons from the $f_{7/2}$ shell to the higher shells. In view of the above discussion, it is worthwhile to investigate the nuclear structure of these nuclei employing a realistic nucleon-nucleon (NN) interaction in a large configuration space of the full *fp* shell.

In the present work we are concerned with the nuclear structure of ^{52}V and ^{53}V. Results of our calculations for lighter vanadium isotopes have already been reported.[8] In the calculations reported here, an inert ^{40}Ca core is assumed and the single particle orbitals $0f_{7/2}$, $1p_{3/2}$, $0f_{5/2}$, and $1p_{1/2}$ are included in the active space. The calculations are performed in the framework of the Hartree-Fock (HF) projection formalism,[9] employing the modified[10] version of the Kuo-Brown effective NN interaction wherein the matrix elements in the $|(f_{7/2})^2 JT\rangle$ states are renormalized to account for the omission of the $g_{9/2}$ orbit included in the original model space of Kuo and Brown.[11] The same effective interaction has been used in our previous work on scandium,[12,13] vanadium,[8,13] and chromium[14] isotopes and was found to reproduce the energy spectra and electromagnetic properties reasonably well. The HF calculations with axially symmetric deformations show that there are many energetically close intrinsic states of the two vanadium nuclei under consideration. This necessitates a band mixing calculation to determine the admixture of various intrinsic states in the nuclear wave function. The nuclear wave functions are, therefore, obtained from the good angular momentum states projected from the individual intrinsic bands by the band-mixing prescription[13] outlined in Sec. II. In the present band-mixing calcula-

γ-ray spectroscopy of excited states in ^{143}Eu

R. Aryaeinejad, R. B. Firestone,* W. H. Bentley, and Wm. C. McHarris

National Superconducting Cyclotron Laboratory, and Departments of Chemistry and Physics, Michigan State University, East Lansing, Michigan 48824

(Received 11 August 1980)

The level structure of the $N = 80$ nucleus ^{143}Eu has been studied by the ^{144}Sm$(p,2n\gamma)^{143}$Eu reaction using a 30-MeV p beam. We have assigned 37 γ rays deexciting 30 states in ^{143}Eu, placed on the basis of excitation functions and γ-γ coincidence information. Angular distributions were taken at 90°, 100°, 110°, 125°, 140°, and 155° with respect to the beam direction, yielding the A_2 and A_4 coefficients. The in-beam experiments tended to excite higher-spin states than those known from existing β-decay data. Taking the various data together, we could make definite J^π assignments for most of the states in ^{143}Eu. Calculations were performed to explain the resulting level structure in terms of a triaxial weak-coupling model for both prolate and oblate deformations. These calculations indicate that ^{143}Eu has a slight oblate deformation.

[NUCLEAR REACTIONS ^{144}Sm$(p,2n\gamma)^{143}$Eu, E_p = 30 MeV; measured E_γ, I_γ, γ-γ coinc, $\sigma(E_\gamma,\theta)$; deduced ^{143}Eu levels J, π; enriched targets, Ge(Li) detectors; triaxial weak-coupling shell-model calculations.]

I. INTRODUCTION

One of the more interesting regions of the nuclidic chart for current study is the region immediately below the $N = 82$ closed shell. Here, long chains of isotones are amenable to study, encompassing both neutron-excess and neutron-deficient nuclei; a wealth of $M4$ and other isomers is available; and a large number of targets is available for cross-comparison in various in-beam experiments. The neutron-deficient $N = 80$ isotones are among the most interesting of these nuclei because, although they are close to the major closed shell, they lie at a considerable distance from stability. Thus, they are transitional nuclei; they contain many well-defined shell-model states, but they lie near the edge of the onset of deformation, so many of their higher-lying states can be characterized not only as multiple particle states, but also as (deformed) collective states. Also, the juxtaposition of the $h_{11/2}$ shell-model state with various low-spin states leads to a wealth of both high- and low-spin states in these nuclei.

We have now completed a series of studies on the three odd-mass $N = 80$ isotones, $^{143}_{63}Eu_{80}$, $^{141}_{61}Pm_{80}$, and $^{139}_{59}Pr_{80}$, by in-beam γ-ray spectroscopy.[1] These supplement and complement our (and other) previous studies of states in these nuclides excited by β^+/ϵ decay (^{143}Eu, Refs. 2–4; ^{141}Pm, Refs. 5 and 6; and ^{139}Pr, Refs. 7 and 8).

In this paper we report our results on states in ^{143}Eu. By using the in-beam techniques we were able to populate many high-spin states not populated by the β^+/ϵ decay. Many experiments such as γ-γ coincidences, excitation functions for the various γ rays, and angular distributions were carried out in order to construct the final level scheme. In the last sections we attempt to explain the experimental level scheme using a triaxial weak-coupling model described by Meyer-ter-Vehn.[9]

II. EXPERIMENT

A. Target and reaction

The states in ^{143}Eu were excited by the ^{144}Sm$(p, 2n\gamma)^{143}$Eu reaction, using a p beam from the Michigan State University (MSU) (50-MeV) sector-focused cyclotron. The target was prepared by vaporizing Sm enriched to 95.10% ^{144}Sm (obtained from Oak Ridge National Laboratory) onto a thin C backing. The target was 200–300 μg/cm^2 thick and the C backing 25 μg/cm^2 thick.

Excitation functions calculated by the compound-nucleus evaporation code ALICE[10] are shown in Fig. 1. From these it can be seen that the primary contaminants produced directly by the 30-MeV p beam were ^{144}Eu, ^{142}Sm, and, to a lesser extent, ^{142}Eu. Their decays also produced readily identifiable γ rays from states in ^{144}Sm, ^{143}Sm, ^{143}Pm, ^{142}Sm, and ^{142}Nd. These predictions were observed in the experiments and accounted for.

B. γ-ray singles spectra

The ^{143}Eu singles γ-ray spectra were taken with a 10% efficient [with respect to a 7.6×7.6-cm NaI (Tl) detector for the ^{60}Co 1332.513-keV peak; source-to-detector distance, 25 cm] Ge(Li) detector having a resolution of 2.4 keV full width at half maximum (FWHM) (for the ^{60}Co 1332.513-keV peak). They were normally taken at an angle of 125° from the beam direction [to minimize ang-

Hole states in the tin isotopes observed by the (p, t) reaction

G. M. Crawley, W. Benenson, G. Bertsch, S. Gales,* D. Weber,† and B. Zwieglinski‡
Physics Department and Cyclotron Laboratory, Michigan State University, East Lansing, Michigan 48824
(Received 25 August 1980)

A broad structure has been observed in (p, t) reactions on the tin isotopes ^{112}Sn, ^{116}Sn, ^{118}Sn, ^{120}Sn, ^{122}Sn, and ^{124}Sn between 7 and 9 MeV of excitation energy. The width of the peak has a minimum of around 1.9 MeV for the reaction ^{116}Sn(p, t) and increases for both the ^{112}Sn(p, t) reaction and for the heavier tin targets, but the excitation energy of the structure increases with mass number. The measured angular distributions of the bump in ^{110}Sn, ^{114}Sn, and ^{120}Sn agree reasonably well with single-step, distorted-wave Born approximation calculations. The widths of the peaks observed in two neutron transfer show the same trends with mass number as the widths of the single hole states observed in one neutron transfer reactions. It appears that the peak contains components which arise from the pickup of one particle from a deep orbit and one particle from a valence orbit, plus possibly some contribution from pickup of two particles from deep orbits.

[NUCLEAR REACTIONS ^{112,116,118,120,122,124}Sn(p,t), ^{117,119}Sn(p,d); $E=42$ MeV; ^{110,114,116,118,120,122}Sn measured E_x, Γ; ^{110,114,120}Sn measured $\sigma(\theta)$. DWBA analysis; enriched targets, resolution 40 keV.]

I. INTRODUCTION

Deep hole states have been observed in a variety of single neutron transfer reactions on the tin isotopes.[1-11] The feature observed consists of one or more broad bumps which are characterized by angular momentum transfers of 4 or 1 and therefore have been identified as holes in the $1g_{9/2}$ and $2p$ orbits. In the present experiment, broad structures were also observed in the triton spectra following proton bombardment of the tin isotopes. Because the two neutrons picked up can couple to various angular momenta, it is not possible to make a unique assignment of orbital angular momentum transfer and so determine from which shell model orbits the neutrons are being picked up. In the present paper a systematic study of the (p, t) reaction on the even even tin isotopes ^{112}Sn, ^{116}Sn, ^{118}Sn, ^{120}Sn, ^{122}Sn, and ^{124}Sn is described. The broad structure is observed in all six isotopes studied, but its width and excitation energy vary from isotope to isotope. Angular distributions have been measured on ^{112}Sn, ^{116}Sn, and ^{122}Sn. A preliminary report of this work has been published.[12]

In order to investigate the systematics of the comparison of the two hole states with single hole states, a few measurements of the (p, d) reaction were made on two odd tin isotopes, ^{117}Sn and ^{119}Sn. Broad features similar to those observed on even-even targets were also observed in these cases.

II. EXPERIMENTAL METHOD

The experiment was carried out using the 42 MeV proton beam from the Michigan State University Isochronous Cyclotron. In the initial work, the tritons were detected using a solid state detector telescope. Because of the limitation in count rate from the elastic peak in the detectors and the presence of dead layers on the solid state detectors, the experiment was transferred to the Enge split-pole spectrograph. The same features were observed with both detection methods. Two different wire counters were used in the focal plane. One was a resistive wire counter, and the other used a delay line readout to fix position.[13] Both counters were backed by a plastic scintillator, and deuterons and tritons were unambiguously identified by their time of flight through the spectrograph and their energy loss in the wire counter. A NaI monitor detector at a fixed laboratory angle of 90° was used to normalize different runs. The absolute cross section was obtained by measuring the elastic scattering at 8°, 10°, and 12° and comparing with an optical model calculation. The calculated elastic cross section is quite insensitive to the particular choice of optical parameters at these forward angles, and thus the absolute cross sections are accurate to better than 10%. One of the largest uncertainties in extracting the cross section for the broad feature arises from the background subtraction. An estimate of this error was made by repeating the extraction of the peak a number of times with different backgrounds. The spread of values obtained for the peak was about 10%.

The tin spectra were calibrated using the known low lying states of the lighter tin isotopes, the oxygen and carbon impurities in the tin targets, and also the ^{58}Ni(p, t) and ^{64}Ni(p, t) reactions. This gave a consistent calibration which was

PHYSICAL REVIEW C VOLUME 23, NUMBER 2 FEBRUARY 1981

Energy levels in ^{23}Mg from the ^{25}Mg$(p,t)^{23}$Mg reaction

H. Nann
Indiana University, Bloomington, Indiana 47405

A. Saha
Northwestern University, Evanston, Illinois 60201

B. H. Wildenthal
Cyclotron Laboratory, Michigan State University, East Lansing, Michigan 48824

(Received 29 September 1980)

Angular distributions of the ^{25}Mg$(p,t)^{23}$Mg reaction have been measured at 40 MeV bombarding energy. An energy resolution of 10–15 keV permitted the observation of about 40 new levels in ^{23}Mg up to 9.72 MeV of excitation. Unambiguous spin and parity assignments of $5/2^+$ are made to the levels at 0.045(3), 5.662(8), 6.566(8), 6.899(5), 6.982(5), 7.582(6), 7.795(6), and 8.155(6) MeV on the basis of an $L = 0$ admixture in the angular distributions. Values of the orbital angular momentum L transferred to several states have been deduced. Microscopic distorted-wave Born approximation calculations for the transitions to the first eight $5/2^+$ states have been performed using spectroscopic amplitudes from recent shell model calculations and are compared to the experimental data.

[NUCLEAR REACTIONS ^{25}Mg(p,t), $E_p = 40$ MeV; measured $\sigma(E_t,\theta)$. ^{23}Mg deduced levels, L, J^π. DWBA analysis. Enriched target.]

I. INTRODUCTION

The level scheme of ^{23}Mg is well established up to an excitation energy of 7.3 MeV.[1] Above this energy only one level at 7.79 MeV is reported in the compilation of Ref. 1. Most recently, an investigation of the ^{24}Mg(p,d) ^{23}Mg reaction at 95 MeV bombarding energy[2] yielded several new levels in ^{23}Mg in the excitation energy range from 7.3 to 13.3 MeV.

The present investigation of the ^{25}Mg$(p,t)^{23}$Mg reaction with better energy resolution than previously obtained was undertaken with the aim of extending the existing information about ^{23}Mg. Angular distributions were obtained from 6° to 60° for approximately 51 out of a total of 77 levels up to an excitation energy of 9.72 MeV. From the observed characteristic shapes of the angular distributions several unique spin assignments were deduced and in other instances limits for spin values were set.

Microscopic distorted-wave Born approximation (DWBA) calculations using spectroscopic amplitudes calculated from the shell-model wave functions of Chung and Wildenthal[3] were performed for the transitions to the first eight $J^\pi = \frac{5}{2}^+$ levels in ^{23}Mg and compared to the experimental data.

II. EXPERIMENTAL PROCEDURE

The ^{25}Mg$(p,t)^{23}$Mg reaction was studied at $E_p = 40$ MeV at the Michigan State University cyclotron. The triton groups were detected in a position-sensitive proportional counter with delay line readout,[4] backed by a plastic scintillator, on the focal plane of an Enge split-pole spectrograph. This detector system provided excellent particle identification and an overall energy resolution between 10 and 15 keV. The target consisted of highly enriched ^{25}Mg (better than 96%) evaporated onto a thin carbon foil. The thickness was about 60 μg/cm^2.

A triton spectrum obtained at a laboratory angle of 6° is shown in Fig. 1. The peaks are labeled by their excitation energies. The spectra were analyzed by a peak-fitting program. Angular distributions were measured from 6° to 60° for transitions to states in ^{23}Mg up to 9.72 MeV of excitation. They are displayed in Figs. 2–7. Error bars reflect only statistical uncertainties. The absolute cross sections were obtained by normalization to the elastic scattering of protons from ^{25}Mg recorded between 25° and 50° under experimental conditions which were identical except for an appropriate adjustment of the spectrograph magnetic field. The measured elastic scattering differential cross sections were assumed to have the values calculated in the optical model from the parameters of Becchetti and Greenlees.[5] The accuracy of the absolute cross section normalization is estimated to be about ± 20%.

III. RESULTS

The excitation energies of the levels observed in the present experiment are collected in Table

Mass of ^{6}Li and the excitation energy of its 3.56-MeV state

R. G. H. Robertson and J. A. Nolen, Jr.
Cyclotron Laboratory and Physics Department, Michigan State University, East Lansing, Michigan 48824

T. Chapuran* and R. Vodhanel
Physics Department, University of Illinois, Champaign, Illinois 61820

(Received 30 October 1980)

The excitation energy of the second excited state of ^{6}Li has been measured to be 3562.88 ± 0.10 keV by comparing the energy of resonance fluorescence radiation from this state to calibration lines from a ^{56}Co source. Also the Q value of the ^{6}Li$(p,\alpha)^3$He reaction has been determined relative to the ^{19}F$(p,\alpha)^{16}$O reaction, giving a result for the ground state mass excess of ^{6}Li of 14 085.5 ± 1.1 keV, somewhat below the tabulated value of 14 087.3 ± 0.8 keV. These measurements improve the sensitivity of experiments searching for isovector parity violation in ^{6}Li.

[NUCLEAR REACTIONS ^{6}Li$(\gamma,\gamma)^6$Li, bremsstrahlung source, E_γ = 3.56 MeV, measured E_γ. Ge(Li) detector. ^{6}Li$(p,\alpha)^3$He, E_p = 10.5 MeV, measured Q. Magnetic spectrograph.]

I. INTRODUCTION

The 0$^+$, T = 1 state of ^{6}Li at 3.56 MeV is energetically able to decay into a deuteron and an alpha particle but is forbidden to do so by conservation of parity and of isospin. A measurement of the decay probability therefore gives a measure specifically of the ΔT = 1 part of the parity-nonconserving interaction. The ^{6}Li case has acquired new significance with the emergence of unified gauge theories of the weak and electromagnetic interactions, which imply the existence of a hadronic weak neutral current. Isovector parity violation is suppressed in conventional descriptions of charged current interactions but is not necessarily suppressed if a hadronic weak neutral current exists.[1]

This decay is now being studied by a group at the Université de Montréal[2], and by a Michigan State University–Argonne National Laboratory–Chalk River Nuclear Laboratory collaboration.[3] In these experiments and several previous ones,[4] the excitation function of the inverse reaction ^{4}He$(d,\gamma)^6$Li or ^{2}H$(\alpha,\gamma)^6$Li is investigated in the region of the 0$^+$, T = 1 state. The presence of parity violation would be indicated by a weak resonance superimposed on the direct capture continuum. A limit to the experimental sensitivity is imposed by the range of energies which must be searched over in order to be certain that the resonance is included. The major contribution to this uncertainty originates in the mass difference between the 0$^+$, T = 1 state of ^{6}Li and ^{4}He + ^{2}H. A direct measurement of this difference to the desired accuracy does not appear to be practical, and in this paper we describe independent measurements of the excitation energy and of the ground state mass of ^{6}Li.

It may be useful at the outset to consider what precision is needed in this program of measurements. A lower limit to the search range in the parity-violation experiment is set by the energy spread and instability of the incident beam. Measurements at Chalk River[3] have demonstrated that, at 6.24 MeV, the energy appropriate for ^{2}H$(\alpha,\gamma)^6$Li via the 3.56-MeV state, a resolution close to 2 keV can be reliably achieved, with an instability less than 1 keV. (The natural and Doppler widths are smaller.) It can be shown that the optimum search range is approximately three times the resolution, or about 6 keV. If one wishes 95% confidence that the resonance lies within the range, then the combined standard deviation in beam energy and masses must be 1.5 keV or less. A beam energy determination to 1 keV is feasible, implying a similar accuracy requirement in the resonance energy. Because of the laboratory-to-center-of-mass kinematic conversion, the precision required in the mass excesses is about 0.3 keV. Neither the ground state mass of ^{6}Li nor the excitation energy of the 3.56-MeV state is known to this accuracy. Two recent measurements[5,6] establish the excitation energy to about 0.5 keV, but there is a serious discrepancy (almost 6 keV) between these results and another of lower precision.[7]

The ground state mass of ^{6}Li has not been determined by direct mass spectroscopic techniques, and its present value (with a quoted uncertainty of

PHYSICAL REVIEW C VOLUME 23, NUMBER 3 MARCH 1981

Fission of ^{238}U induced by inelastic scattering of 120 MeV α particles

B. B. Back
Argonne National Laboratory, Argonne, Illinois 60439

A. C. Shotter,* T. J. M. Symons, and A. Bice
Lawrence Berkeley Laboratory, Berkeley, California 94720

C. K. Gelbke, T. C. Awes, and D. K. Scott
Michigan State University, East Lansing, Michigan 48824
and Lawrence Berkeley Laboratory, Berkeley, California 94720

(Received 8 September 1980)

The fission decay of ^{238}U has been measured as a function of excitation energy in inelastic scattering of 120 MeV α particles. Total kinetic energies and masses of fission fragments were measured by the double energy method. It is observed that the total kinetic energy E_K decreases and that the valley in the mass distribution is reduced when the excitation energy of the system is increased. No indication of anomalous total kinetic energy release in the region of the giant quadrupole resonance has been found. A qualitative interpretation of the data is given on the basis of a static scission point model.

[NUCLEAR REACTIONS, FISSION ^{238}U$(\alpha,\alpha' f)$, $E=120$ MeV, $\theta_\alpha=16°$; measured total kinetic energy and fission fragment mass distributions as a function of excitation energy.]

I. INTRODUCTION

One of the long standing questions in fission research is concerned with the descent from the saddle point to scission. Whether the available energy is transferred into internal degrees of freedom or into relative motion of the two nascent fragments prior to scission is still largely unknown, since measurements of final parameters of the reaction do not directly address the question of the dynamical evolution of the fission decay.

However, some success in explaining many of the features of fission has been obtained with a static model[1] of the scission point configuration, which takes into account the shell structure in the nascent fragment. Most prominently, it appears that the deformed shell for $A=138$ is responsible for the strongly asymmetric mass distributions in fission of most actinide elements. A strong spherical shell closure at $Z=50$, $N=82$ is believed to be associated with the decrease of the total kinetic energy with excitation energy as observed in several light ion and neutron induced reactions on uranium and plutonium targets.[2-6]

To further study this latter correlation, we have measured the fission decay of ^{238}U induced by the (α,α') reaction. We find that the total kinetic energy decreases with excitation energy at a rate of $dE_K/dE^* = -0.38 \pm 0.07$ and that the effect is concentrated in the heavy fragment mass region of $M_H = 125-135$.

II. EXPERIMENTAL PROCEDURE AND DATA ANALYSIS

A beam of 120 MeV α particles from the 88" cyclotron at Lawrence Berkeley Laboratory was used to bombard a 530 μg/cm^2 thick, self-supporting metallic ^{238}U target. Inelastically scattered α particles were identified in a triple telescope of solid state detectors located at $\theta=16°$ out of the horizontal plane. Two fission detectors were placed at $\theta=90°$ and $\theta=-90°$ in the horizontal plane, each subtending a solid angle of $\Omega_f \simeq 440$ msr. Coincident events between the telescope and the two fission detectors were recorded on magnetic tape for subsequent analysis.

The elements of the detector telescope were gain matched by introducing a calibrated charge pulse on the detector side of the preamplifiers. The energy calibration was obtained from the elastic peak in the α spectrum. The fission detectors were energy calibrated with the fission fragments from a thin ^{252}Cf source.[7]

The data were analyzed off line by an event-by-event reconstruction of the kinematics. Identification of α particles in the telescope was obtained by generating a particle identification spectrum from the measured pulse heights in each element in the detector telescope and selecting events in the peak corresponding to α particles. The primary energies and masses of the fission fragments were calculated by an iterative procedure, taking

States in odd-odd ^{116}Sb excited by the decay of ^{116}Te

C. B. Morgan,* W. H. Bentley, R. A. Warner,† and W. H. Kelly‡
Heavy Ion Laboratory and Department of Physics, Michigan State University, East Lansing, Michigan 48824

Wm. C. McHarris
Heavy Ion Laboratory, Department of Chemistry, and Department of Physics, Michigan State University, East Lansing, Michigan 48824
(Received 19 November 1980)

Gamma-ray spectroscopic experiments have been performed on the β^+/ϵ decay of 2.50-h ^{116}Te. Results from these experiments and from complementary in-beam γ-ray angular distributions were used to construct a decay scheme. Twenty-one γ rays were identified and placed in the decay scheme containing states in ^{116}Sb at 0 ($J^\pi = 3^+$), 93.7 (1^+), 103.0 (2^+), 446.0 (3), 550.9 (2), 574.4 (2), 731.7 (1^+), 917.7 (1^+), and 1158.3 (1^+) keV. The structures of the odd-odd Sb states are analyzed and discussed in simple shell-model terms.

[RADIOACTIVITY ^{116}Te [from ^{116}Sn(^{3}He,3n)^{116}Te]; measured E_γ, I_γ, deduced α_K, α_{tot}; deduced logft; ^{116}Sb deduced levels, J, π; Ge(Li) singles and γ-γ coinc.; shell-model considerations.]

I. INTRODUCTION

Odd-odd nuclei can provide a convenient and useful means of examining the p-n residual interaction. Because of the general complexity of odd-odd states, it is the odd-odd nuclei close to closed shells, where the single-nucleon components of the wave functions are amenable to shell-model analysis, that are the most practicable for study. Because of the relatively low amounts of energy available for populating odd-odd states by the β decay of their even-even neighbors, the best sources of information supplement radioactivity studies with in-beam experiments.

We have embarked upon a series of in-beam experiments using the $(p,n\gamma)$ reaction on nuclei near the $Z=50$ shell,[1] including populating and examining states in the odd-odd nucleus $^{116}_{51}Sb_{65}$. Since we discovered that the results of previous experiments on the β decay of ^{116}Te conflicted with the in-beam results and because of the complementary nature of the decay studies, we undertook a reinvestigation of ^{116}Te decay, which we report in this paper.

The identification and study of 2.50 ± 0.02-h ^{116}Te has a fairly spotty history[2-6]—for a summary of the early results, cf., Ref. 2. The basic previous work on the decay of ^{116}Te to states in ^{116}Sb remains that of Fink, Andersson, and Kantele[2] [magnetic conversion-electron and β^+ studies plus NaI(Tl) γ-ray studies, including γ-γ coincidences]. Subsequent Ge(Li) γ-ray studies[7,8] and magnetic conversion-electron studies[9] have proven less reliable. In this paper we present what we believe to be the first complete and comprehensive ^{116}Te decay scheme, based primarily on Ge(Li) γ-ray singles and γ-γ coincidence data, but also making free and extensive use of our in-beam angular correlation data[1] to facilitate making J^π assignments and to determine the more detailed structures of the states. We conclude with an examination of the structures of the lower-lying states in simple shell-model terms.

II. DESCRIPTIONS OF EXPERIMENTS

A. Source preparation

Samples of 95% enriched ^{116}Sn (obtained from Oak Ridge National Laboratory) in the form of powdered SnO_2 were contained in Al foil envelopes and bombarded with a 32-MeV ^{3}He beam from the Michigan State University Sector-Focused Cyclotron. The 32-MeV beam was chosen on the basis of excitation function calculations with the computer code CS8N,[10] which predicted that the cross section for the ^{116}Sn(^{3}He,3n)^{116}Te reaction would peak at that energy. [Q values for the (^{3}He,3n) and (^{3}He,4n) reactions are −15.66 and −26.80 MeV, respectively.]

Following 30-60-min bombardments, the ^{116}Te sources were aged for ≈ 30 min to allow the shorter-lived contaminants to decay away. The sources were then transferred to fresh Al foil envelopes for counting. Typically, three of four such sources were used to accumulate spectra having adequate statistics.

B. γ-ray singles experiments

The γ-ray singles spectra were obtained with an 18% efficient [relative to a 7.6×7.6-cm^2 NaI

PHYSICAL REVIEW C VOLUME 23, NUMBER 4 APRIL 1981

^{194,196,198}Pt(p,p') reactions at 35 MeV

P. T. Deason,* C. H. King,† R. M. Ronningen, T. L. Khoo,‡ F. M. Bernthal, and J. A. Nolen, Jr.
Departments of Chemistry and Physics and Cyclotron Laboratory, Michigan State University, East Lansing, Michigan 48824
(Received 14 October 1980)

The ^{194,196,198}Pt(p,p') reactions have been studied at a proton energy of 35 MeV using nuclear emulsion plates and a high-resolution position-sensitive proportional counter. Approximately 45 levels were populated in each reaction. In ^{198}Pt, 38 of 44 levels to about 3.2 MeV are reported for the first time. Angular distributions from 20° to 110° were measured for many of these levels. Several new J^π assignments were made using empirical shapes of transitions to well-known levels in Pt. The results for the $J^\pi = 0^+, 2^+, 4^+$, and (for ^{194}Pt) 6^+ members of the ground band and the 2^+, 3^+, and 4^+ members of the "quasi-γ" band were analyzed by coupled channels calculations incorporating relative transition strengths from the interacting boson approximation model. The multipole moments of the deformed optical model potential were calculated and compared to moments deduced from other studies.

[NUCLEAR REACTIONS ^{194}Pt(p,p'), ^{196}Pt(p,p'), ^{198}Pt(p,p'), E_p = 35 MeV; measured $\sigma(E_p,\theta)$; deduced energies, J^π; coupled channels calculations, interacting boson approximation model; deduced optical model and deformation parameters, quadrupole and hexadecapole moments; comparisons to Coulomb excitation, (α,α'), and (^{12}C, ^{12}C′); enriched targets, nuclear emulsion plates (7 keV FWHM) and position-sensitive proportional counter (15 keV FWHM), magnetic spectrograph.]

I. INTRODUCTION

The transitional region between the well-deformed rare-earth nuclei and the spherical nuclei near ^{208}Pb has been rather intractable to application of traditional models of collective motion. Until recently, most of the properties of the lowest-lying states could be understood only after numerical solution[1-3] of the full collective Hamiltonian. Recently a simpler picture, the interacting boson approximation (IBA) model of Arima and Iachello,[4] has evolved. This model has its origin in the group symmetry properties of those identical nucleon (or nucleon hole) pairs in angular momentum states of $L=0$ or $L=2$ which are outside closed shells. The simplest geometrical models, the vibrational and rotational limits of the collective model, approximately correspond to possible subgroups [SU(5) and SU(3), respectively] for which the IBA Hamiltonian, having SU(6) group symmetry, might be symmetric. In the Os-Pt region the subgroup O(6) has been shown by Cizewski *et al.*[5] to account for most of the energy and decay properties of all positive parity levels in ^{196}Pt below the pairing gap. Taking ^{196}Pt as the best example of O(6) symmetry the lighter mass even-even Os and Pt nuclei might be understood by breaking the O(6) symmetry with the introduction of a quadrupole-quadrupole interaction which introduces deformation to the nucleus.

The tests of the IBA model in its O(6) symmetry that have now been made in the Pt nuclei include those by Cizewski *et al.*[5] who have studied the gamma decay properties, and those by Deason *et al.*[6] who have searched for low-lying $J^\pi = 0^+$ levels in ^{192,194,196}Pt using high resolution (p,t) reactions. Both studies located many new levels and found the O(6) limit predictions of branching ratios, level energies, and two-particle transfer strengths in good agreement with experiment.

Our present study of ^{194,196,198}Pt using the (p,p') reaction at 35 MeV also provides level energy and spin-parity information on these nuclei. Inelastic scattering is one of the few ways to study the most neutron-rich stable isotopes, such as ^{198}Pt. (Previously, only six levels in ^{198}Pt were known,[7-9] and precise energies were known for only two of these.) The (p,p') reaction at 35 MeV is selective, can reach high spin ($J \approx 8$), and can be studied with high resolution (2–8 keV, using nuclear emulsion plates). Additionally, proton inelastic scattering angular distributions contain nuclear shape information. In this study we report on the population of approximately 45–50 levels in each nucleus to about 3 MeV excitation and the measurements of their energies. We use empirical shapes of angular distributions for excitations of levels with known J^π to make new J^π assignments. We then use relative matrix elements from the O(6) limit of the IBA model in a coupled channels approach in an attempt to describe the angular distributions for the low-lying levels. The parameters of the deformed optical model potential used in the coupled channels calculations are optimized to fit

Alpha particle emission in peripheral heavy ion reactions at 20 MeV/u

M. Bini
Physics Department, University of Florence, Florence, Italy
and Lawrence Berkeley Laboratory, Berkeley, California 94720

C. K. Gelbke and D. K. Scott
Cyclotron Laboratory, Michigan State University, East Lansing, Michigan 48824
and Lawrence Berkeley Laboratory, Berkeley, California 94720

T. J. M. Symons, P. Doll,* D. L. Hendrie, J. L. Laville,† J. Mahoney, M. C. Mermaz,‡ C. Olmer,§ K. Van Bibber,‖ and H. H. Wieman
Lawrence Berkeley Laboratory, Berkeley, California 94720
(Received 12 May 1980)

The reaction ^{197}Au(^{16}O,HIα) has been investigated at 310 MeV. The angular correlations of alpha particles measured in coincidence with projectile-like fragments are very strongly forward peaked; the reaction is dominated by large negative values of the three-body Q value. Most of the observed alpha particles are emitted from projectile-like fragments. Within a factor of 2, no anisotropy of emission in the center-of-mass frame of the coincident projectile residue and alpha particle was found.

[NUCLEAR REACTIONS ^{197}Au(^{16}O, HIα), E=310 MeV; measured two-dimensional HI-α coincident energy and angular correlations; deduced reaction mechanisms.]

I. INTRODUCTION

From the numerous recent experimental and theoretical studies of light particle emission in heavy-ion collisions, it has become clear that these particles are an important source of information on the time evolution of the reaction mechanism from low energies close to the Coulomb barrier up to the highest available relativistic energies. Over the whole energy domain, there is an increasing emphasis on coincidence measurements, which refine the global insights derived from the earlier single particle inclusive experiments. In this paper we discuss such coincidence measurements between alpha particles and projectile-like fragments in reactions induced by ^{16}O on ^{197}Au at 310 MeV. This energy lies in the transitional region between low and high energy heavy-ion phenomena.[1] Some initial results of the experiments were reported earlier.[2]

At low energies, less than 5 MeV/u above the Coulomb barrier, the interaction time of the two colliding nuclei is longer than, or comparable to, the nuclear relaxation time of typically 10^{-21} sec.[3-7] The dominant reaction mechanisms are established as deeply inelastic scattering or compound nucleus formation (see Refs. 3–7 and references therein). Here, the light particles are primarily emitted from the compound nucleus or from the fully accelerated and statistically equilibrated nuclei formed in deeply inelastic collisions.[8-11] Strictly speaking, these conclusions are based on studies of heavy colliding nuclei ($A \geq 40$). For lighter nuclei, there is already evidence for a component of preequilibrium emission of light particles, even at energies below 5 MeV/u.[12,13]

At higher energies, an increased, or even dominant, contribution is expected from preequilibrium processes, as established already in light-ion induced reactions.[14-18] The decrease in the reaction time allows the excitation of higher lying states, which subsequently decay by particle emission rather than propagate into more complicated configurations. This possibility is less likely in low energy heavy-ion collisions, where the energy loss in each step is too small to lead to significant preequilibrium emission.[19] There exists now a substantial body of data which demonstrate that nonequilibrium, light particle emission is an important aspect of heavy-ion collisions between 5 and 10 MeV/u, not only for deeply inelastic scattering[20-32] but also for incomplete fusion reactions.[25,33-39]

In spite of the wide variety of observed phenomena, a common feature in the experiments is the observation of angular correlations between alpha particles and projectile-like fragments that are not symmetric about the direction of the outgoing projectile residue. This asymmetry has been attributed to the emission of light particles from the contact zone between the two nuclei, prior to the subsequent deeply inelastic or fusion reaction. In a few cases,[40-42] evidence for this

Core excitations in ^{63}Cu by the ^{63}Cu$(p,p')^{63}$Cu and ^{65}Cu$(p,t)^{63}$Cu reactions

Y. Iwasaki,* G. M. Crawley, and J. E. Finck
Cyclotron Laboratory, Michigan State University, East Lansing, Michigan 48824
(Received 30 December 1980)

Core excitations up to $E_x = 4$ MeV in ^{63}Cu have been studied by the reactions ^{63}Cu$(p,p')^{63}$Cu and ^{65}Cu$(p,t)^{63}$Cu at 40 MeV proton energy. The transferred angular momentum L has been determined for each transition on the basis of the angular distribution shape. A quartet-plus-doublet pattern is consistently observed for the groups of states corresponding to the 2_1^+, 3_1^-, and 4_1^+ states of the core nucleus ^{62}Ni. This implies the existence of doublets arising from the coupling of collective states of the core with the $2p_{1/2}$ proton orbital, in addition to the quartets from the coupling with the $2p_{3/2}$ proton orbital considered in the conventional weak-coupling excited-core model. It is pointed out that the existence of a weak-coupling situation cannot be proved only on the basis of transfer-reaction data, and in this regard the importance of a comparative study of the inelastic-scattering and transfer-reaction data is emphasized.

[NUCLEAR REACTIONS ^{65}Cu$(p,t)^{63}$Cu and ^{63}Cu$(p,p')^{63}$Cu, $E = 40$ MeV; measured E_x and $\sigma(\theta)$, determined L. Resolution 16 keV for the (p,t), 20 keV for the (p,p'). Enriched targets. Deduced excited-core multiplets.]

I. INTRODUCTION

Low-lying states in a number of spherical, odd nuclei have been interpreted in terms of the particle- (hole-) core-coupling picture[1,2] or the particle- (hole-) vibration-coupling picture.[3,4] The nucleus ^{63}Cu is a typical example of such nuclei. In the particle-core-coupling picture, the nucleus ^{63}Cu consists of one proton added to the proton-closed-shell nucleus ^{62}Ni which is called the core.[2,5] Inelastic scattering has been shown to be an effective means of selectively exciting collective degrees of freedom of the core.[6-9] More recently, the ^{65}Cu$(p,t)^{63}$Cu reaction was used to study the quadrupole excited-core components of low-lying states in ^{63}Cu.[10,11] The (p,t) reaction on an odd-proton target nucleus is a very appropriate tool for studying core excitations, since the state of the odd proton is kept unchanged to first order during this reaction process.[10]

While the (p,t) and inelastic scattering reactions have much in common as a means of core excitation, they provide different kinds of information, because they have essentially different reaction mechanisms. Therefore, a comparative study of the (p,t) reaction and the inelastic scattering leading to the same final nucleus may give new insights into core excitations and the particle-core-coupling in an odd-proton nucleus.

Previous experiments have studied the (p,p') or (p,t) reaction separately. For example, angular distributions of differential cross sections for the ^{63}Cu$(p,p')^{63}$Cu reaction were previously measured at $E_p = 17.5$ MeV (Ref. 9) and lower energies.[6,12] In addition, the ^{65}Cu$(p,t)^{63}$Cu reaction has been studied at $E_p = 19.5$ MeV (Ref. 11) and 51.9 MeV.[10] However, the present paper reports a comparative study of these two reactions for the first time. The present experimental study also has better energy resolution and covers a larger range of excitation energy in ^{63}Cu than the previous experiments.

II. EXPERIMENTAL PROCEDURE

The reactions ^{65}Cu$(p,t)^{63}$Cu and ^{63}Cu$(p,p')^{63}$Cu have been studied at the incident proton energy of 40 MeV using the Michigan State University Isochronous Cyclotron. The particles from the target were detected by a delay-line counter[13] placed on the focal plane of the Enge split-pole magnetic spectrograph. Time-of-flight and energy-loss signals were used for particle selection.

A. ^{65}Cu$(p,t)^{63}$Cu

Differential cross sections for the ^{65}Cu$(p,t)^{63}$Cu reaction were measured over the laboratory angular range of 6° through 64°. The target was a self-supporting metallic foil of ^{65}Cu with a thickness of 250 μg/cm^2. The overall energy resolution was 16 keV. Figure 1 shows a typical spectrum. There is practically no background.

B. ^{63}Cu$(p,p')^{63}$Cu

Differential cross sections for the proton inelastic scattering by ^{63}Cu were measured over the laboratory angular range of 8° through 95°. The target was a self-supporting metallic foil of ^{63}Cu with a thickness of 520 μg/cm^2. The overall

Nuclear Physics A348 (1980) 493–517;

PION-CONDENSED NUCLEAR MATTER AT FINITE TEMPERATURES

P. HECKING

Cyclotron Laboratory, Michigan State University, East Lansing, Mich. 48824, USA

Received 11 June 1979

Abstract: The possibility of density isomers in nuclear matter, induced by pion condensation, is discussed with special regard to heavy-ion collisions. The equation of state of the combined system of baryons and pions is treated within the framework of the linear σ-model. In dense baryon matter, such as in colliding nuclei at high energies, the state with a non-zero value of the static pion field $\langle\pi\rangle$ might become energetically favorable due to the attractive p-wave pion-nucleon interaction. We present results for the shift, due to the pion condensation, of the free and internal energy and of the pressure at finite temperatures up to $k_B T \sim 100$ MeV. Repulsive short-range baryon-baryon correlations in the pion-like channel, $\Delta(1232)$ isobar admixtures to the nucleons as well as finite-range pion-baryon vertex cutoffs are taken into account. The influence of various "reference" equations of state – adjusted to the equilibrium properties of nuclear matter in the uncondensed phase – on the density isomerism is discussed. The results for the critical density ρ_c, above which pion condensation is expected, are compared with calculations based on the singularities of the pion propagator $D(k, \rho, \omega, T)$ in a dense medium.

1. Introduction

A considerable number of publications [1–6]) discuss the possibility of symmetric nuclear matter as well as neutron matter undergoing a phase transition into a "pion-condensed" phase above a critical nucleon density. This state, qualitatively different from normal nucleon matter, is characterized by a macroscopically occupied pion-phase coexisting with the baryons. The discussion of this behavior of dense matter has been motivated from two sides:

(i) From high-energy heavy-ion reactions [7–9]) one can possibly get information about the properties of nuclear matter at densities 2–4 times larger than the nuclear density $\rho_0 = 0.17\,\mathrm{fm}^{-3}$. The existence of a pion-condensate might favor the coherent production of pions which could be seen by the Hanbury-Brown-Twiss effect [10]). Speculations about the modulation of the nuclear density induced by a pion-condensate [1]) have also been made.

(ii) A pion-condensate probably has a drastic influence on the properties of a neutron star, especially on its cooling [11–14]).

Further interest has focused on the connection between density isomerism and shock-wave dynamics [7,8]) as well as the possible existence of quasistable superdense nuclei [15]). It should be noted that density isomerism was also suggested in connection with the transition from normal to "abnormal" nuclear matter [16]) with a strongly

Nuclear Physics A350 (1980) 227–252

THE MAGNETIC FORM FACTOR OF ^{3}He†

D.O. RISKA

Department of Physics, Michigan State University, East Lansing, Michigan 48824, USA

Received 9 June 1980

Abstract: The behavior of the magnetic form factor of ^{3}He for momentum transfers $q^2 < 30$ fm^{-2} is studied with simple wave function models and with account of pion and ρ-meson exchange current effects. The single-nucleon current contribution to the form factor depends strongly on the D-state probability. The exchange current contributions dominate the form factor for $q^2 > 5$ fm^{-2}. The sensitivity of the exchange current contributions to wave function details – short-range correlations and D-state percentage – and hadronic form factors in the exchange operators is investigated in some detail. With inclusion of the ρ-meson exchange effect the predicted position of the form factor minimum is in reasonable agreement with the most recent data. With the exchange effects considered the predicted magnetic moment agrees with the empirical value. The models employed lead to no noticeable difference in the behavior of the triton and helion magnetic form factors.

1. Introduction

That meson exchange currents play a large role in magnetic electron scattering is by now widely realized. Yet there are only few known instances in which the exchange current contributions completely dominate the scattering cross sections already at moderately small values of momentum transfer. These are the cross section for backward electrodisintegration of the deuteron near threshold [1]) and the magnetic form factors of the three-body systems [2,3]). The main reason for the exchange current dominance in these particular observables is the strong destructive interference between the S- and D-state matrix elements of the single-nucleon current operator which makes the impulse approximation contribution small. This exchange current dominance makes these observables uniquely suited for detailed study of the exchange current effects themselves.

The situation is best understood in the case of backward deuteron electrodisintegration. Here theoretical calculations [1,4,5]) are in good agreement with data as far as data are available [6,7]). The reason is of course the possibility of constructing the deuteron and np scattering wave functions explicitly from realistic models for the nuclear force. In the three-body systems the situation is understood only in a qualitative sense, although the failure of the impulse approximation to account for the magnetic form factors (and magnetic moments) is well established by the work of Brandenburg *et al.* [2]) and Harper *et al.* [8]) That pion exchange currents can compensate for most of this deficiency has been shown by Barroso and Hadjimichael [3]). In

† Research supported in part by the National Science Foundation.

Nuclear Physics **A352** (1981) 221 – 236;

ENERGY DEPENDENCE IN PROTON INELASTIC SCATTERING *

R. A. MOYER † and R. W. FINLAY
Department of Physics, Ohio University Athens, Ohio 45701, USA

and

G. M. CRAWLEY
Cyclotron Laboratory, Michigan State University East Lansing, Michigan 48824, USA

Received 6 August 1980

Abstract: Differential elastic and inelastic scattering of protons from ^{92}Mo was investigated under conditions chosen to emphasize the energy dependence of the cross sections in the region from 25–45 MeV. Elastic scattering data are described in terms of an optical-model potential with energy-dependent potential-well depths and constant geometrical parameters. Inelastic scattering cross sections are calculated in distorted-wave Born approximation with form factors given by the vibrational model for five low-lying eigenstates. Apart from a possible anomaly at the lowest energy studied, no evidence was obtained for an explicit dependence of deformation length on incident proton energy. The sensitivity of the deformation lengths to the details of the analysis is discussed.

E NUCLEAR REACTIONS ^{92}Mo(p, p), (p, p'), E = 24.89, 29.84, 34.90, 45.30 MeV; measured $\sigma(\theta)$; deduced optical-model parameters. ^{92}Mo levels deduced deformation lengths. Magnetic spectrometer, enriched target.

1. Introduction

Inelastic scattering of nucleons from spherical even-even nuclei can be described by a vibrational model in which the nuclear shape is allowed to oscillate about a spherical mean. The projectile-nucleus optical-model potential is assumed to follow the shape of the nucleus. The non-spherical parts of the potential are able to induce transitions to these vibrational states. The spherical parts of the potential may be determined by fitting the elastic scattering data thus fixing the radial shape of the inelastic scattering interaction. Inelastic cross sections are calculated in distorted-wave Born approximation (DWBA) and are scaled to fit the data. The scaling factor for a transition to a final state with $J, \pi = L, (-1)^L$ is $\delta_L^2 = (\beta_L R)^2$ where δ is the deformation length and β_L is the deformation parameter. If the deformations are

* Supported by grants PHY 7822696 and PHY 7809911 from the National Science Foundation.
† Present address: Department of Nuclear Engineering, University of Wisconsin, Madison, Wisconsin.

Nuclear Physics A355 (1981) 207–220;

FIRST STUDY OF THE (^{14}C, ^{12}C) REACTION
Selectivity of the reaction and the energy levels of ^{28}Mg and ^{30}Si

F. POUGHEON, M. BERNAS, M. ROY-STEPHAN, C. DÉTRAZ, D. GUILLEMAUD, E. KASHY †, M. LANGEVIN, F. NAULIN and P. ROUSSEL
Institut de Physique Nucléaire, BP no. 1, 91406 Orsay, France

Received 22 May 1980
(Revised 7 October 1980)

Abstract: The first measurements are reported for (^{14}C, ^{12}C) two-neutron stripping reactions. Energy spectra up to an excitation energy of 12 MeV have been measured at 69 MeV for the ^{26}Mg(^{14}C, ^{12}C) and ^{28}Si(^{14}C, ^{12}C) reactions. A strong selectivity of this reaction is observed. Using this selectivity, the comparison of the spectra suggests J^{π} assignments for several ^{30}Si and ^{28}Mg states. The results from the other two-neutron stripping reactions, (t, p) and (^{18}O, ^{16}O) are compared with those of the (^{14}C, ^{12}C) reaction.

E NUCLEAR REACTIONS ^{26}Mg, ^{28}Si(^{14}C, ^{12}C), E = 69 MeV; measured $\sigma(\theta)$. ^{28}Mg, ^{30}Si deduced levels, J, π. Enriched targets.

1. Introduction

A new attractive field has been opened recently with the ability of accelerating ^{14}C beams. Among the new light heavy-ion projectiles, ^{14}C is the lightest $T = 1$ projectile available that can be used in investigating two-nucleon transfer reactions such as two-proton pickup (^{14}C, ^{16}O) and two-neutron stripping (^{14}C, ^{12}C). It also provides a new entrance channel for exotic transfer reactions used to measure the mass and energy spectra of unknown nuclei far from the stability valley [1,2]. The first results reported on the (^{14}C, ^{16}O) reaction have shown it to be valuable for studying proton pair correlations in medium-mass nuclei [3].

The two-neutron stripping reaction has been studied with light ions using the (t, p) reaction and recently through the (α, ^{2}He) reaction on 1p and 2s-1d shell nuclei [4,5]. Since heavy-ion induced reactions have specific properties, like the strong dynamic effects on the selectivity of the populated levels and the importance

† Permanent address: Cyclotron Laboratory, Michigan State University East Lansing, Michigan 48824, USA. Supported in part by NSF-PHY 7822696.

Nuclear Instruments and Methods 179 (1981) 119–124

ON IMPROVING Ge DETECTOR ENERGY RESOLUTION AND PEAK-TO-COMPTON RATIOS BY PULSE-SHAPE DISCRIMINATION *

N. MATSUSHITA, Wm.C. McHARRIS, R.B. FIRESTONE **, J. KASAGI and W.H. KELLY ***
National Superconducting Cyclotron Laboratory and Departments of Chemistry and Physics, Michigan State University, East Lansing, Michigan 48824, USA

Received 1 April 1980

The rise-time discrimination of pulses from Ge detectors can be used to improve the spectra on two levels: first, by discriminating against slower-rising pulses, both the energy resolution and peak-to-Compton ratios can be improved significantly, especially for detectors that have suffered neutron damage. Second, by adding a pulse-height correction to compensate for effects of varying rise-time, an improved composite spectrum can be obtained without significant loss in detector efficiency.

1. Introduction

Since the introduction in the early 1960s of semiconductor detectors for γ-ray spectroscopy, almost constant efforts have been expended to improve both their energy resolution and their peak-to-Compton ratios [1], to some extent mutually incompatible goals. For example, the larger the detector, the better the peak-to-Compton ratio, but also, in general, the poorer its resolution. And such panaceas as very large volume intrinsic Ge detectors [2] or successful fabrication of detectors from semiconductors having both a high Z and a small band gap † (e.g. InSb) have not yet appeared on the scene. Thus, we often find a necessary compromise: a Ge(Li) γ-ray detector with the best energy resolution practicable (and often of medium to small size) used in conjunction with one of the more or less elaborate Compton-suppression spectrometers [4,5] which are necessarily expensive, cumbersome and require elaborate coincidence electronics.

An additional concern arises when Ge(Li) detectors have been used for in-beam γ-ray experiments. Here they often suffer from neutron damage, viz., the neutrons cause lattice defects in the Ge crystals, which act as traps for the charge carriers [1,6,7]. These trapping centers not only contribute to poorer resolution because of incomplete charge collection, but also they slow down the rate of charge collection [7]. Thus, in general, poorer resolution should also be associated with pulses having slower than normal rise times. By discriminating against these pulses we should be able to improve the effective resolution of a detector, albeit at the expense of some efficiency.

We report here on some startling early results we have obtained for improving the energy resolution and the peak-to-Compton ratio for several small Ge and moderate-sized Ge(Li) detectors of differing configurations. Our original quest was to find out more about the rise times of varying signals from Ge and Ge(Li) detectors and to seek ways to improve the resolution of neutron-damaged detectors. (Some earlier work has been reported in connection with the rise times of pulses from semiconductor detectors, both for Si(Li) [8] and for Ge(Li) [9] detectors. However, the details of rise-time and pulse-height relationships were not investigated.)

We were indeed able to improve the resolution and peak-to-Compton ratios significantly: we can improve the resolution of our "typical" detector by approximately 50%, the exact amount depending on the amount of neutron damage the detector has suffered. For a brand new, state-of-the-art, high-resolution

* This material is based on work supported by the US National Science Foundation under Grant No. PHY 78-01684.
** Present Address: Nuclear Science Division, Lawrence Berkeley Laboratory, Berkeley, Calif. 94720, USA.
*** Present Address: Office of the Dean, Montana State University, Bozeman, Montana 59717, USA.
† For a summary of the present state-of-the-art with respect to certain "exotic" detector materials see ref. [3].

Nuclear Instruments and Methods 180 (1981) 285–304

MAGNETIC FIELD MAPPING OF THE K-500 CYCLOTRON AT M.S.U *

G. BELLOMO, D.A. JOHNSON, P. MILLER and F.G. RESMINI
Cyclotron Laboratory, Michigan State University, East Lansing, Michigan, U.S.A.

Received 24 September 1980

The results of an extensive magnetic field mapping of the K-500 cyclotron under construction at M.S.U., covering the entire operating range of the machine, are reported. The data are analyzed in detail, and a comparison with the theoretical calculations used in designing the cyclotron is carried out. This comparison allows one to draw some general conclusions on the reliability of the theoretical model and its implications for superconducting cyclotron design.

1. Introduction

The purpose of this paper is to report the results of an extensive magnetic field mapping of the three sector K-500 cyclotron under construction at MSU [1]. The measurements were intended to:
– provide a detailed picture of the variations of the iron-produced field, both for the azimuthal modulation and the average field, over the entire operating range of the cyclotron;
– allow a comparison with previous calculations, so as to establish the reliability of the latter;
– check the existence of imperfections;
– determine if modifications of the pole tip geometry were needed in order to achieve the appropriate field for the cyclotron.

This paper deals with the first three topics, since field corrections and its trimming are extensively reported elsewhere [2]. All maps were taken using the field measuring apparatus described in ref. 3. For the present purposes we may just recall that 54 flip-coils are spaced at 0.5″ intervals from 0″ to 26.5″ radius, along a radially positioned bar, so that all data corresponding to a given azimuth are taken at once, by flipping the coils twice throught 180°. Azimuthal intervals were 2° for all maps. The entire data-taking process (flipping-storage-azimuthal movement) is computer controlled and typically a 360° map in 2° intervals takes about four and a half hours. The overall precision of the measurements, taking into account calibration errors, temperature corrections, etc. is about ±0.03%. While this was judged entirely adequate for the present purposes, several improvements are planned for later mappings with the final field configuration in order to bring the error down to ±0.01%.

* This material is based upon work supported by the National Science. Foundation under Grant No. Phy 78-22696 and Department of Energy DE-AC02-80ER10579.

2. Pole geometry

We shall briefly review the pole geometry relevant to these field maps. It differs from the one used in earlier field measurements [3] only by the presence of the center plug, which has been designed to allow the insertion of the internal source.

2.1. Pole tip geometry

A perspective view of a hill and a valley is given in fig. 1, while the radial profiles relative to the median plane are given in fig. 2. The pole radius is 25.75″, but the iron structure, as shown clearly in fig. 1, continues as part of the inner tank wall from 26″ to 28″ radius both for the hill and the valley. There is therefore a 1/4″ radial gap between the two iron structures. A central hole of 3.5″ radius is provided for the plug insertion.

The upper part of the hill, 5.75″ thick, is flat, providing a 2.5″ constant axial gap between 3.5″ and 25.75″ radius, and has an average spiral constant of 1/13 (rad/inch). The hill is actually machined into two pieces in order to approximate the said spiral

Nuclear Instruments and Methods 180 (1981) 305–318

TRIMMING OF THE MAGNETIC FIELD FOR THE K-500 CYCLOTRON AT M.S.U. *

G. BELLOMO and F.G. RESMINI
Cyclotron Laboratory, Michigan State University, East Lansing, MI 48824, U.S.A.

Received 24 September 1980

The expected final characteristics of the magnetic field of the K-500 cyclotron at MSU are presented, together with the procedure used to properly shape and trim the field. The equilibrium orbits' properties of a number of representative ions are also given and discussed in detail.

1. Introduction

Following an extensive magnetic field mapping of the three-sector K-500 cyclotron under construction at MSU [1], and whose results are reported in ref. 2, it appeared that various field corrections were necessary in order to achieve the desired properties of the cyclotron in terms of axial focusing and isochronism, while keeping the trim-coil power within reasonably l w limits. A number of alterations of the iron configuration were also needed for construction reasons, as will be seen in the following.

This paper describes the corrections to the pole tip geometry which were decided and their effects on the field. Upon this basis we then analyze the expected cyclotron performance in terms of the equilibrium orbit properties for a number of representative ions, and the overall trim coils requirements throughout the operating range of the machine.

2. The uncorrected pole tip geometry

For the present purposes it is useful to recall the main features of the coils and pole tip geometry.

A perspective view of a hill and a valley for the uncorrected geometry is given in fig. 1, while their profiles relative to the median plane are sketched in fig. 2. The pole radius is 25.75″, but the iron structure, as shown in fig. 1, continues as a part of the inner tank wall from 26″ to 28″ radius, both for the hill and the valley. There is a 0.25″ gap between the two structures. The upper part of the hill is 5.75″ thick, and it is the one around which the trim coils will be wound. The gap in the hill region is uniformly 2.5″, the spiral constant 1/13 rad/inch. The azimuthal hill width starts from 33° at 3.5″ radius and reaches 46° at 10″, being thereafter essentially constant up to 25.75″. The hill shoe inserted in the tank wall is instead 60° wide as noted in fig. 2.

All essential features of the valleys are represented in self-explanatory way in fig. 2.

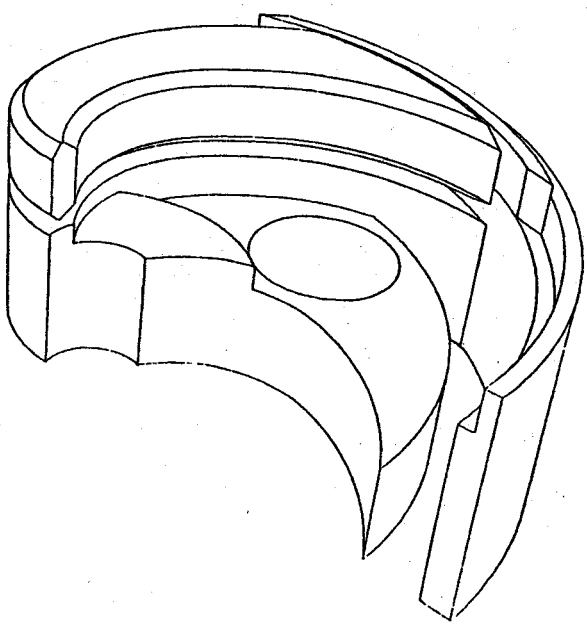

Fig. 1. Perpective view of a sector for the K-500 pole tip geometry.

* This material is based upon work supported by the National Science Foundation under Grant No. Phy 78-22696 and Department of Energy DE-AC02-80ER10579.

Nuclear Instruments and Methods 180 (1981) 319–333

A SURVEY OF BEAM DYNAMICS PRIOR TO EXTRACTION IN THE K-500 CYCLOTRON AT M.S.U. *

E. FABRICI and F.G. RESMINI
Cyclotron Laboratory, Michigan State University, East Lansing, MI 48824, U.S.A.

Received 24 September 1980

This paper presents a detailed study of the accelerated beams dynamics, prior to extraction, for the K-500 cyclotron under construction at M.S.U. The results, for a number of representative beams, indicate that adequate turn to turn separation can be achieved, while keeping distortions to a substantially negligible level. The presence of the $\nu_R + 2\nu_Z = 3$ resonance, and its effect in limiting the cyclotron dynamic range is also discussed.

1. Introduction

The present analysis of beam dynamics for the M.S.U. K-500 superconducting cyclotron has the main goal of establishing the conditions under which proper turn separation can be achieved at extraction radius, while preserving the necessary beam quality in phase space.

Excitation of the $\nu_R = 1$ resonance, as in conventional A.V.F. cyclotrons, looks the only viable method. Consequently, the amplitude and phase of the field first harmonic needed to excite the resonance, and of those inherently present in the field because of the magnetic channels used in the extraction, have been carefully investigated.

This study was carried out, using very realistic and perfectly isochronized magnetic fields, on a set of eight representative ions spanning the entire cyclotron operating range both in terms of the charge to mass ratio and the magnetic field level. A brief review of the calculation methods and the general properties of the magnetic field is given below.

2. General outline and calculations methods

We shall use these notations:

Z/A = charge to mass ratio (electron charge/amu) of the accelerated particles,

B_0 = nominal center field value, usually in kG, for which isochronism has been calculated,

T/A = ion energy in MeV/n.

The customary notation ν_R and ν_Z shall be used for the radial and axial focusing frequencies respectively, while the rf frequency is denoted by ν_{RF}. Its harmonic number with respect to the particle orbital frequency is h.

It is useful to recall some features of the pole tip geometry of the machine. Hills and valleys, following a spiral law with 1/13 (rad/inch) constant, are shown in fig. 1 together with the extraction scheme. The azimuthal scale is also shown, in order to help relating the azimuth values, given in the following, to the actual pole geometry. More details on the latter are given in refs. 1 and 2.

All the calculations reported here use very realistic magnetic field maps, i.e. obtained from measured data by the method described in detail in ref. 2.

The average field is properly isochronized with a least square fitting procedure. The latter uses both the main coils and trim coils, and takes into account the actual variation, as a function of the main coils currents, of the field generated by the iron configuration. The azimuthal step of a map is 1°, thus allowing Runge–Kutta integration at 2° intervals. The radial step size is 0.5".

Equilibrium orbit properties are derived via the equilibrium orbit code, on field maps having three-fold-120° symmetry. Accelerated orbits are tracked with the code SPIRAL-GAP [3], generally on 360° maps. The latter are obtained by superposing to the 120° maps the calculated perturbing effects of the

* This material is based upon work supported by the National Science Foundation under Grant No. Phy 78-22696 and Department of Energy DE-AC02-80ER10579.

Nuclear Instruments and Methods 180 (1981) 335–341

TRANSPORT DE FAISCEAU POUR SPECTROSCOPIE IONS LOURDS A HAUTE RESOLUTION

P. ROUSSEL et E. KASHY *
Institut de Physique Nucléaire, B.P. n° 1, 91406 Orsay Cédex, France

Reçu le 21 avril 1980 et en forme revisée le 23 septembre 1980

A method is given to adjust a beam-transport system to the requirements of high energy-resolution heavy ion spectroscopy. The results of a test experiment performed on a MP tandem with a ^{12}C beam are shown. A drastic improvement in energy resolution is obtained for a kinematical factor $K = (1/p)\,dp/d\theta \sim 0.12$.

1. Introduction

Lorsqu'une réaction à deux corps est utilisée en physique nucléaire, la résolution en énergie est souvent une question cruciale. Cela reste vrai pour l'étude de la diffusion élastique: il faut être capable d'isoler le fondamental du 1er niveau excité, ce qui peut être difficile à grande énergie incidente. Pour les réactions induites par ions lourds, deux facteurs contribuent à limiter la résolution en énergie: les phénomènes de cible et le facteur cinématique $[K = (1/p)\,dp/d\theta]$. L'évolution de ces deux facteurs avec l'énergie incidente est différente: dans la cible, la dispersion de perte d'énergie ("straggling") est sensiblement indépendante de l'énergie incidente tandis que la perte d'énergie elle-même décroit quand l'énergie incidente croit. Au contraire, l'effet du facteur cinématique (strictement constant en valeur relative, pour un bilan d'énergie de la réaction nul) va augmenter avec l'énergie et va devenir déterminant aux très grandes énergies incidentes; nous ne nous intéresserons ici qu'à ce dernier.

Lorsqu'un spectromètre magnétique est utilisé, il est bien connu [1] que l'existence d'un facteur cinématique K conduit à placer le détecteur dans un plan focal "déplacé", différent du plan focal "vrai" correspondant à une source radioactive ($K = 0$). On peut aussi reconstituer les trajectoires [2] et calculer leur intersection avec le plan focal déplacé. Pour une ouverture angulaire importante, on ne peut d'ailleurs plus négliger le terme d'ordre 2 ($d^2p/d\theta^2$) et la reconstitution devient nécessaire pour tenir compte de la variation de K avec θ, à l'intérieur de la plage angulaire utilisée.

Mais ces opérations ne sont suffisantes que pour un faisceau incident idéal, d'émittance nulle. Pour un faisceau réel, en effet, on observe nécessairement sur la cible une dispersion des points d'impacts (abscisse x_c), des angles d'incidence (θ_c) et des impulsions incidentes $[\delta_c = 100(\delta - \delta_0)/\delta_0]$ (voir appendice A pour les notations) et cela va conduire à une dispersion des points d'impact des trajectoires sortantes, dans le plan focal déplacé.

Il est possible d'exprimer au premier ordre, la position du point d'impact dans le plan focal déplacé en fonction des paramètres x_i, θ_i, δ_i de la trajectoire *au début* du système de transport de faisceau [3]. Si le calcul par matrices est utilisé, il suffit en effet d'insérer au niveau de la cible la matrice représentant (au 1er ordre) l'effet de la réaction nucléaire (voir appendice A). On peut alors annuler simultanément la contribution des termes en θ_i et δ_i (il subsiste bien sûr le terme en x_i) en introduisant sur la cible une corrélation position/angle et position/énergie. Ces corrélations sont produites [4] en focalisant le faisceau en aval de la cible et en imposant à cet endroit une valeur déterminée à la dispersion linéaire (R_{16}).

Ces phénomènes sont assez bien connus dans leur principe et des résultats ont déjà été publiés en ions légers [5,6] (seule intervient alors l'adaptation des dispersions) et ce court article a pour but d'indiquer une procédure de leur mise en application et de donner les résultats (spectaculaires) correspondants, obtenus lors d'une expérience test, en *ions lourds*, sur une ligne de faisceau standard, auprès du tandem d'Orsay.

* Adresse parmanente: Michigan State University, East Lansing, U.S.A. (soutenu en partie par NSF-PHY-7822696).

Nuclear Instruments and Methods 184 (1981) 301–318
North-Holland Publishing Company

THE EXTRACTION SYSTEM FOR THE K-500 CYCLOTRON AT M.S.U. *

E. FABRICI, D. JOHNSON and F.G. RESMINI
Michigan State University, East Lansing, Michigan 48824, U.S.A.

Received 24 September 1980

The final design features of the extraction system for the K-500 cyclotron under construction at MSU are presented. The resulting cyclotron performance for a number of typical ions are reviewed and the expected extracted beam phase space characteristics are also discussed.

1. Introduction

This paper reports the final design features of the K-500 cyclotron extraction system, under construction at MSU, as of March 1980. It differs in several aspects, especially contruction-wise, from schemes reported earlier [1] and it seems worthwhile to review in some detail the rationale for the present choices and the expected performances.

As described in ref. 1 the system consists of electrostatic deflectors, followed by several magnetic channels of the passive type i.e. made with bars of saturated iron. The main changes introduced are:
– all elements, i.e. deflectors and channels, are radially movable;
– the number of electrostatic deflectors has been reduced from three to two;
– the number of magnetic channels has been increased to eight;
– a magnetic channel has been inserted in the traversal of the yoke.

The modifications stemmed out of a careful analysis of the internal and extracted beam dynamics for several representative ions which cover the entire operating range of the cyclotron. Realistic field maps, with properly isochronized fields as described in ref. 2, were used throughout. Since detailed studies of the internal beam dynamics are reported elsewhere [3], we shall only concern ourselves here with the characteristics and performance of the extraction system itself.

* This material is based upon work supported by the National Science Foundation under Grant No. Phy 78-22696 and Department of Energy DE-AC02-80ER10579.

0029-554X/81/0000–0000/$02.50

2. Layout and design features

The pole tip geometry, together with the layout of the extraction system, is schematically presented in fig. 1. Shown are the hills contours, including the hill shoe, 60° wide, and positioned in the inner tank wall from 26″ to 27″ in radius [2]. All the azimuths referred to in this paper are according to the scale of fig. 1.

We shall first give a general description of the extraction scheme, analyzing later in detail the single components.

2.1. Main characteristics

All the elements shown in fig. 1 are also listed in table 1 together with their main parameters. The entries in table 1 are as follows:

E, M, C	= characterizes an electrostatic deflector, a magnetic channel or a compensating bar respectively.
θ_I, θ_F	= initial and final azimuth of the element as referred to in fig. 1.
$\bar{R}_I, \bar{R}_F$	= average central ray radius at the initial and final azimuth of each element.
ΔR	= range of radial movement for each element around the average position.
$E_{max}, B, \partial B/\partial x$	= maximum electric field for deflectors, bias magnetic field and gradient for the magnetic channels.

Two electrostatic deflectors, the first one 55°

Nuclear Instruments and Methods 186 (1981) 435–440
North-Holland Publishing Company

A REACTION PRODUCT MASS SEPARATOR FOR ENERGETIC PARTICLES AT MSU

L.H. HARWOOD and J.A. NOLEN, Jr.
National Superconducting Cyclotron Laboratory, Michigan State University, East Lansing, Michigan 48824, USA

A reaction product mass separator which has been designed and is under construction at the National Superconducting Cyclotron Laboratory (Michigan State University) is described. Unslowed reaction products emerging from the target are dispersed according to their mass-to-charge ratio (m/q) and focused to points on a focal plane. The prototype system will transmit particles in the 1–30 MeV/u range. The design of a system for up to 200 MeV/u is also discussed. The types of experiments to be done are given as well.

1. Introduction

A major area of nuclear physics is the study of exotic nuclei, i.e. nuclei far from the valley of β-stability. Production of exotic nuclei and their subsequent study has often been hampered by limitations in beam energy or intensity. Studies of exotic nuclei have also suffered from high background radiation levels, low detection efficiencies, etc. To overcome these last problems and take advantage of the beams at the new Michigan State University heavy-ion cyclotron facility a Reaction Product Mass Separator (RPMS) [1, 2] has been designed and is being constructed. This device is described below as are current plans for a second RPMS capable of accepting higher energy particles, up to 200 MeV/u.

2. Basic concept

In order to study the decay of exotic nuclei it is desirable to have them separated from the beam and other sources of radiation so that the detection system can operate in a friendly environment. Also, having the exotic nuclei concentrated spatially is advantageous to minimize the size of the detectors needed and to enhance the signal-to-noise ratio. Finally, the more exotic the nucleus is, the shorter (on the average) is its lifetime. Hence, fast transit times are desirable so that the nuclei do not decay before they can be studied. One often-used device in such studies is the conventional on-line mass separator [3]. Such separators have certain limitations, however. Because the reaction products must be stopped, thermalized, reionized, and accelerated, the study of nuclear levels is limited to those with lifetimes of at least 10–100 ms, thereby precluding those with lifetimes in the millisecond range and isomers in the microsecond range. The other major problem with ion sources is their sensitivity to the chemical nature of the ions. The chemistry of the nuclei can change a system's sensitivity greatly. For example, the alkali metals are easily ionized and thus produce good ion beams; refractory elements, on the other hand, are hard to ionize and are harder to make into ion beams. Great progress has been made in the production of "difficult" ion beams, but the chemical sensitivity problem still remains.

The ion source can be eliminated from the system by focusing the products directly as they leave the target. One such device, called the EMS (energy-mass spectrometer) [4], has been built by the MIT group at Brookhaven National Laboratory. This device disperses vertically in velocity and horizontally in momentum thereby creating slanted lines of constant mass-to-charge ratio. This device retains excellent momentum resolution, but does not cencentrate the yield of a given m/q species into a small detection volume. Hence, this system is more suited for reaction mechanism studies than for decay studies of low yield reaction products. The Lohengrin fission-product separator at Grenoble is somewhat similar in concept to the EMS, however, and it has been used for decay studies [5, 6].

0029-554X/81/0000-0000/$02.50

Particle Accelerators
1980 Vol.11 pp.161–172
0031-2460/81/1103-0161$06.50/0

ELECTRIC FOCUSING IN CYCLOTRONS WITH UNUSUAL DEES*

M. M. GORDON and FELIX MARTI

Cyclotron Laboratory, Michigan State University, East Lansing, Michigan 48824 U.S.A.

(Received October 7, 1980)

Previous analyses of electric focusing are reviewed and found to be restricted to cyclotrons with 180° dees. For dees with smaller angular widths, an alternating-gradient type of focusing occurs because the ions generally enter and exit each dee on opposite sides of the rf voltage peak. This AG focusing effect is analyzed and formulas are derived for calculating the resultant change in ν_z. These formulas are applied first to the MSU superconducting cyclotron, which has three 60° dees, and then to the Indiana cyclotron which has two 38° dees. We find in the first case that electric focusing will be quite significant for certain harmonics, and in the second case that it may even produce a small region of vertical instability through overfocusing. Next, the analysis of Dutto and Craddock is generalized so as to apply to dees with spiral electric gaps like those designed for use in superconducting cyclotrons. Formulas for the resultant change in both ν_r and ν_z are derived, and then applied to the MSU cyclotron with some rather interesting results.

1. INTRODUCTION

During electric gap-crossings, ions in the beam experience vertical focusing forces produced by the same rf field that is responsible for their acceleration. This electric focusing plays an important role near the center of most cyclotrons in a region where the magnetic focusing tends to be very weak and where, simultaneously, the defocusing associated with space-charge repulsion has its greatest strength.

The focusing effects produced by the rf electric field in classical cyclotrons were analyzed first by Rose[1] and Wilson,[2] and later with some refinements by Cohen.[3] Since then, this analysis has been revised and extended to isochronous cyclotrons by a number of authors.[4,5] As a result, most aspects of the phenomena are now well understood.

Before proceeding, it seems worthwhile to review briefly some important properties of electric focusing. First, the time dependence of the forces leads inevitably to a vertical acceptance for the cyclotron that depends on the phase of the injected ions (whether from an internal or external source). Moreover, it turns out that this phase dependence differs substantially from that of the energy gain per turn.

These conflicting characteristics tend to limit considerably the phase acceptance, as well as the vertical acceptance of most cyclotrons. Within these limitations, the ultimate performance can nevertheless be significantly improved by means of suitable design procedures, as pointed out by several investigators.[6]

To understand the basic phenomena, one should first recognize the electric lenses which accelerate ions across a gap generally produce a focusing impulse as the ions enter the gap and a defocusing one as they exit. These opposing impulses result from the curvature of the electric field lines, which is illustrated, for example, in Fig. 1.

The primary focusing effect in cyclotrons, called the "phase effect", is produced by the time variation of the dee voltage. Here for example, if the ion crosses the gap at a time when the field strength is falling, then the focusing impulse will exceed the defocusing one, and a net focusing will result. Conversely, if the crossing occurs when the field strength is rising, then a net defocusing is produced. This phase effect turns out to be inversely proportional to the turn number, and moreover, the result is essentially independent of the electric-field variation within the gap.

The secondary focusing effects in cyclotrons are almost exactly the same as those associated with static electric lenses. These are the well-known "acceleration" effect and the "thick-lens" effect, which always yield a net focusing

* This material is based on work supported by the National Science Foundation under Grant No. Phy 78-22696.

Ann. Rev. Nucl. Part. Sci. 1980. 30: 383–436

LARGE-SCALE SHELL-MODEL CALCULATIONS[1] *5621

J. B. McGrory[2]
Physics Division, Oak Ridge National Laboratory, Oak Ridge, Tennessee 37830; and Institute for Theoretical Physics, University of Frankfurt, Frankfurt, West Germany

B. H. Wildenthal[3]
Cyclotron Laboratory, Michigan State University, East Lansing, Michigan 48824

CONTENTS

[2] Research sponsored by the Division of Basic Energy Sciences, US Department of Energy, under contract W-7405-eng-26 with the Union Carbide Corporation.

[3] Research sponsored in part by US National Science Foundation, Grant PHY-7822696.

Journal of General Microbiology (1980), **119**, 217–223. *Printed in Great Britain*

The Reduction of Nitrate to Ammonium by a *Clostridium* sp. Isolated from Soil

By WILLIAM H. CASKEY[1]† AND JAMES M. TIEDJE[2]*

[1] *Department of Microbiology and Public Health, Michigan State University, East Lansing, Michigan* 48824, *U.S.A.*

[2] *Department of Microbiology and Public Health and Department of Crop and Soil Sciences, Michigan State University, East Lansing, Michigan* 48824, *U.S.A.*

(*Received* 11 *September* 1979; *revised* 7 *December* 1979)

Cultures of *Clostridium* KDHS2 reduced $^{15}NO_3^-$ to $^{15}NH_4^+$ with a concurrent increase in molar growth yield of 15·7% compared with fermentatively grown bacteria. The bacteria exhibited a K_s (NO_3^-) of 0·5 mM and reduced NO_3^- maximally at a rate of 0·1 μmol h^{-1} (mg dry wt)$^{-1}$. A partially purified nitrate reductase was obtained which had a K_m (NO_3^-) of 0·15 mM. The reduction of $^{13}NO_3^-$ to $^{13}NH_4^+$ by resting bacteria was not inhibited by NH_4^+, glutamate, glutamine, methionine sulphoximine or azaserine. Glutamine synthetase affected neither the synthesis nor the activity of the NO_3^--reducing enzymes. The results are consistent with the hypothesis that NO_3^- reduction to NH_4^+ in this *Clostridium* sp. is dissimilative. SO_3^{2-}, but not SO_4^{2-}, inhibited the reaction, apparently at the level of NO_2^- reduction.

INTRODUCTION

In anaerobic environments, denitrification is generally considered to be the principal pathway of NO_3^- reduction. Although evidence is sparse, significant quantities of NO_3^- are reduced to NH_4^+ in flooded soils (MacRae *et al.*, 1968) and sediments (Keeney *et al.*, 1971; Koike & Hattori, 1978; Sørensen, 1978). Although NH_4^+ production from NO_3^- has not been observed typically in anaerobically incubated agricultural soils (Bremner & Shaw, 1958; Nommik, 1956; Wijler & Delwiche, 1954), Buresh & Patrick (1978) reported NH_4^+ production under such conditions, and correlation of increased NO_3^- reduction to NH_4^+ with increased amounts of available carbon has been observed recently (Stanford *et al.*, 1975*a*, *b*), suggesting that the potential for NH_4^+ formation exists in such soils. Caskey & Tiedje (1979) presented evidence that NH_4^+ was produced through the activity of spore-forming bacteria, principally *Clostridium* species, via a dissimilatory pathway. A clearer understanding of the physiology of these NO_3^--reducing bacteria may reveal approaches which can be used to predict the occurrence of NO_3^- reduction to NH_4^+, or possibly to enhance this nitrogen-conserving process in agricultural soils.

Comparative fermentation balances and measurements of Y_{ATP} with and without NO_3^- have provided evidence for the dissimilatory function of NO_3^- reduction in *Clostridium* spp. (Hasan & Hall, 1975, 1977). However, reliable measurements of the extent of NO_3^- reduction by these bacteria are lacking. Furthermore, little information is available about the regulation of NO_3^- reduction by *Clostridium* spp. The present study, in addition to providing definitive balances of NO_3^- reduction to NH_4^+, presents evidence that the NO_3^--reducing system of *Clostridium* KDHS2 shares no regulatory features with assimilatory nitrate reductases.

† Present address: Institute of Ecology, University of Georgia, Athens, Georgia 30602, U.S.A.

0022-1287/80/0000-8953 $02.00

Arch Microbiol (1981) 129:135–140

Archives of
Microbiology

Assimilatory Nitrate Uptake in *Pseudomonas fluorescens* Studied Using Nitrogen-13

Michael R. Betlach[1], James M. Tiedje[2], and Richard B. Firestone[3]

[1] Department of Microbiology and Public Health,
[2] Departments of Microbiology and Public Health and Crop and Soil Sciences, and
[3] Cyclotron Laboratory, Michigan State University, East Lansing, Michigan 48824, USA

Abstract. The mechanism of nitrate uptake for assimilation in procaryotes is not known. We used the radioactive isotope, ^{13}N as NO_3^-, to study this process in a prevalent soil bacterium, *Pseudomonas fluorescens*. Cultures grown on ammonium sulfate or ammonium nitrate failed to take up labeled nitrate, indicating ammonium repressed synthesis of the assimilatory enzymes. Cultures grown on nitrite or under ammonium limitation had measurable nitrate reductase activity, indicating that the assimilatory enzymes need not be induced by nitrate. In cultures with an active nitrate reductase, the form of ^{13}N internally was ammonium and amino acids; the amino acid labeling pattern indicated that $^{13}NO_3^-$ was assimilated via glutamine synthetase and glutamate synthase. Cultures grown on tungstate to inactivate the reductase concentrated NO_3^- at least sixfold. Chlorate had no effect on nitrate transport or assimilation, nor on reduction in cell-free extracts. Ammonium inhibited nitrate uptake in cells with and without active nitrate reductases, but had no effect on cell-free nitrate reduction, indicating the site of inhibition was nitrate transport into the cytoplasm. Nitrate assimilation in cells grown on nitrate and nitrate uptake into cells grown with tungstate on nitrite both followed Michaelis-Menten kinetics with similar K_m values, 7 μM. Both azide and cyanide inhibited nitrate assimilation. Our findings suggest that *Pseudomonas fluorescens* can take up nitrate via active transport and that nitrate assimilation is both inhibited and repressed by ammonium.

Key words: *Pseudomonas fluorescens* – Assimilatory nitrate reduction – Nitrate reductase – Nitrate uptake – Active transport – Nitrogen-13 – Short-lived isotope

Many genera of bacteria can assimilate nitrate (Hall 1978), but only a few have been examined to determine the mechanism of assimilation or its regulatory control (Brown et al. 1975; Guerrero et al. 1973; Sias and Ingraham 1979, van't Riet et al. 1968). In pseudomonads, growth on nitrate resembles growth under ammonium limitation: incorporation of inorganic nitrogen into amino acids is catalyzed by glutamine synthetase and glutamate synthase, rather than by glutamate dehydrogenase (Brown et al. 1975). Growth at non-limiting ammonium concentrations represses nitrate assimilation (Brown et al. 1975; van't Riet et al. 1968) as well as the glutamine synthetase-glutamate synthase pathway. More extensive investigations of nitrate assimilation in eucaryotes (for instance, Zumft 1976) indicate glutamine is the true repressor (Dunn-Coleman et al. 1979; Premakumar et al. 1979) and provide evidence for active transport of nitrate into the cells (Goldsmith et al. 1973; Schloemer and Garrett 1974).

The mechanism of nitrate transport during assimilation by bacteria is not known. In dissimilatory nitrate reduction, chlorate, a nitrate analog, has little effect on nitrate reduction in intact bacteria but competitively inhibits the process in inside-out membrane vesicles (John 1977). Whether the nitrate carrier apparently responsible for chlorate exclusion in intact cells is part of an active transport system has not been determined. However, after examining pH transients in response to nitrate pulses in intact cells, Kristjansson et al. (1978) concluded that transport of the nitrate anion during denitrification occurred by facilitated diffusion through a proton symport. They believed the diffusion gradient was maintained by the rapid internal reduction of nitrate to nitrite, which then diffused out of the cells.

Colorimetric procedures and the stable isotope ^{15}N have been used to monitor nitrate uptake, but such procedures lack the sensitivity to resolve rapid time-dependent events, such as inhibition of assimilation, or to monitor the movement of NO_3^--N into the organic N pool. Availability of a radioactive N tracer would alleviate many of the difficulties encountered with the use of ^{15}N. The longest-lived radionuclide of nitrogen, ^{13}N has a half-life of only 10 min and so can be detected in amounts 10^{-10} less than required for ^{15}N mass spectrometry (Tiedje et al., Use of nitrogen-13 in studies of denitrification, Advances in Chemistry, Amer. Chem. Soc., in press). Recent development of procedures to use ^{13}N for studies of nitrogen fixation (Thomas et al. 1975) and denitrification (Tiedje et al. 1979) has provided access to this sensitive tracer to examine nitrogen assimilation. We report here on studies in which $^{13}NO_3^-$ was used to investigate the mechanism of nitrate transport and assimilation in *Pseudomonas fluorescens*.

Materials and Methods

Organism and Growth Medium

The strain of *Pseudomonas fluorescens* used (isolate 72) is representative of the dominant group of denitrifiers in soils and was isolated by Gamble et al. 1978. This strain has been submitted to the American Type Culture Collection. The growth medium contained 50 mM glucose; 50 mM

Present addresses: [1] Extraterrestrial Research Div., NASA Ames Research Center, Moffett Field, California 94035, and [3] Lawrence Berkeley Laboratory, Berkeley, California 94720, USA
Offprint requests to: J. M. Tiedje

0302-8933/81/0129/0135/$01.00

APPLIED AND ENVIRONMENTAL MICROBIOLOGY, Jan. 1980, p. 105-108
0099-2240/80/01-0105/04$02.00/0 Vol. 39, No. 1

Inhibition by Sulfide of Nitric and Nitrous Oxide Reduction by Denitrifying *Pseudomonas fluorescens*†

JAN SØRENSEN,[1]‡ JAMES M. TIEDJE,[1]* AND RICHARD B. FIRESTONE[2]

Department of Crop and Soil Sciences,[1] Department of Microbiology and Public Health,[1] and Heavy Ion Laboratory,[2] Michigan State University, East Lansing, Michigan 48824

The influence of low redox potentials and H_2S on NO and N_2O reduction by resting cells of denitrifying *Pseudomonas fluorescens* was studied. Hydrogen sulfide and Ti(III) were added to achieve redox potentials near −200 mV. The control without reductant had a redox potential near +200 mV. Production of ^{13}NO, $[^{13}N]N_2O$, and $[^{13}N]N_2$ from $^{13}NO_3^-$ and $^{13}NO_2^-$ was followed. Total gas production was similar for all three treatments. The accumulation of ^{13}NO was most significant in the presence of sulfide. A parallel control with autoclaved cells indicated that the ^{13}NO production was largely biological. The sulfide inhibition was more dramatic at the level of N_2O reduction; $[^{13}N]N_2O$ became the major product instead of $[^{13}N]N_2$, the dominant product when either no reductant or Ti(III) was present. The results indicate that the specific action of sulfide rather than the low redox potential caused a partial inhibition of NO reduction and a strong inhibition of N_2O reduction in denitrifying cells.

In a search of environmental factors that influence the overall activity and the differential release of gas products during denitrification, reference is most often given to parameters such as O_2, available carbon, pH, and temperature (2). Much less attention has been paid to the parameters characteristic of the reduced environment, e.g., iron and sulfur compounds. In some environments, in particular marine sediments, denitrification takes place in close proximity to zones of active transformation of iron and sulfur.

In an earlier study in coastal marine sediments, significant accumulation of the denitrification intermediates, NO and N_2O, was noted in the redox transition zone near the sulfide-rich deeper layers; it was suggested that these accumulations were caused by either the low redox potential or the presence of sulfide in this zone (5).

The present study was undertaken to establish whether a low redox potential or the presence of sulfide caused accumulation of NO, N_2O, or both. It was found that sulfide and not a low redox potential caused an increase in proportion of N_2O and NO at the expense of N_2 in denitrifying *Pseudomonas fluorescens*.

MATERIALS AND METHODS

The denitrifying bacterium used was *P. fluorescens* (strain 72), isolated from poorly drained Minnesota maize soil by Gamble et al. (3). The organism was grown anaerobically in tryptic soy or nutrient broth (Difco) with nitrate (3.5 mM KNO_3) or nitrite (5 mM KNO_2) as the electron acceptor. The cells were harvested at early stationary phase by centrifugation at 5°C. Cells were washed three times in 0.02 M phosphate buffer (pH 7.0) and suspended to an optical density of 0.2 to 0.5 at 660 nm.

It was anticipated that gas samples taken in syringes might be subject to O_2 contamination during the short wait before injection into the ^{13}N detection system. This risk was minimized by the admission of excess, unlabeled NO into the syringes, a step which also improved the elution of ^{13}NO from the chromatographic column. The possible lack of a quantitative recovery of ^{13}NO should not exclude a relative comparison of ^{13}NO production between the individual treatments, since all samples of a given incubation time were treated in a similar manner.

Any loss of free sulfide was negligible during the experimental time of 5 min, since a significant decrease of H_2S in similar incubations could not be detected by iodine titration until several hours had elapsed (Sørensen, unpublished data). Both reducing agents provided a measured redox potential (Eh value) near −200 mV. The reaction mixtures without reducing agent gave a positive but variable Eh value between +100 and +300 mV. It was likely that the short exposure to air during the redox assay gave values that overestimated the actual Eh during the incubation. The possible error was less important in the present context, however, where comparisons were made to the strongly reduced series with Ti(III) or H_2S and Eh values near −200 mV.

Five milliliters of the cell suspension was transferred to 25-ml serum vials with 1 ml of a 1% glucose solution. The vials were capped, made anaerobic by repeated evacuation, and purged with helium gas. This proce-

† Journal Article no. 5059 of the Michigan Agricultural Experiment Station.

‡ Present address: Institute of Ecology and Genetics, University of Aarhus, DK-8000-Aarhus, Denmark.

APPLIED AND ENVIRONMENTAL MICROBIOLOGY, Mar. 1981, p. 705-709
0099-2240/81/030705-05$02.00/0
Vol. 41, No. 3

Dissimilatory Reduction of Nitrate and Nitrite in the Bovine Rumen: Nitrous Oxide Production and Effect of Acetylene†

HEINRICH F. KASPAR‡ AND JAMES M. TIEDJE*

Departments of Crop and Soil Sciences[2] and of Microbiology and Public Health,[1] Michigan State University, East Lansing, Michigan 48824

^{15}N tracer methods and gas chromatography coupled to an electron capture detector were used to investigate dissimilatory reduction of nitrate and nitrite by the rumen microbiota of a fistulated cow. Ammonium was the only ^{15}N-labeled end product of quantitative significance. Only traces of nitrous oxide were detected as a product of nitrate reduction; but in experiments with nitrite, up to 0.3% of the added nitrogen accumulated as nitrous oxide, but it was not further reduced. Furthermore, when $^{13}NO_3^-$ was incubated with rumen microbiota virtually no $[^{13}N]N_2$ was produced. Acetylene partially inhibited the reduction of nitrite to ammonium as well as the formation of nitrous oxide. It is suggested that in the rumen ecosystem nitrous oxide is a byproduct of dissimilatory nitrite reduction to ammonium rather than a product of denitrification and that the latter process is absent from the rumen habitat.

Nitrate poisoning of cattle has long been known (11), but little is known about the mechanisms and diversity of microbial transformations of nitrogen oxides in the rumen ecosystem. Lewis (10) first determined ammonium to be the principal terminal product of nitrate reduction in the rumen. Jones (5) noted the accumulation of small amounts of nitrous oxide during 3-day incubations of enrichment cultures started with a heavy inoculum of rumen fluid; he interpreted this as evidence of denitrification. It is now clear that a number of non-denitrifying organisms also can produce N_2O during nitrate reduction (15; J. M. Tiedje et al., Agron. Abstr., p. 165, 1979), and thus the interpretation that denitrification occurs in the rumen may not be correct.

In the present study we report on the quantitative importance and the mechanism of gaseous nitrogen production during dissimilatory nitrogen metabolism in the rumen ecosystem. The effect of acetylene on dissimilatory nitrite reduction to ammonium and nitrous oxide is also shown.

MATERIALS AND METHODS

Materials. Rumen contents were withdrawn before morning feeding from a fistulated Holstein cow fed 5.5 kg of grain and 1.8 kg of hay. The contents were strained through cheesecloth into a bottle which was capped to exclude air and immediately brought to the laboratory. Sodium nitrate (56.75 atom% ^{15}N) and sodium nitrite (96.60 atom% ^{15}N) were obtained from Mound Laboratories, Miamisburg, Ohio and Prochem, Summit, N.J., respectively. All gases used had at least 99.9% purity (Matheson, Joliet, Ill.).

Experiments. Freshly obtained rumen liquor (60 ml) was transferred to a 125-ml Erlenmeyer flask with a septum-capped sidearm. The flask was then connected to an assay system (6) which allowed a thorough exchange between gaseous and liquid phases as well as frequent gas and liquid sampling under anaerobic conditions. Briefly, the apparatus consisted of a gas pump, a gas chromatograph with sampling loop, and a flowmeter, so that the headspace gas could be continuously circulated through the rumen liquor and the gas sampling loop. The rumen liquor was further agitated by a magnetic stirrer. Foaming was prevented by adding 0.1 ml of antifoam solution whenever necessary (antifoam A, 1:500 plus one drop of Tween 80 per 25 ml). After connection of the sidearm flask with the assay system, the gas space was sparged through a vent valve with 95% Ar/5% CH_4 until all air was removed as verified by gas chromatograph analysis for O_2 (6). The vent valve was closed, and for the following 5 min the system was allowed to equilibrate. Then a gas sample (0.1 ml) was taken, and after another 5 min 1 ml of nitrate or nitrite solution was added by means of a syringe through the sidearm septum. Immediately afterwards, two liquid samples (1 ml) were withdrawn by syringe, transferred to test tubes, and frozen in liquid nitrogen. Gaseous and liquid samples were taken every 10 to 15 min until termination of the experiment. The liquid samples were stored in the freezer until analyzed. The experiments were performed at 22°C and atmospheric pressure. The pH of the rumen liquor was 6.9 before and 7.2 after the experiments. The ammonium content of the fresh fluid was 8.8 mM. Samples were pasteurized or sterilized by exposing them to 70 and 120°C, respectively, for 30 min.

Analysis. (i) Nitrous oxide. Gas samples were taken by means of a 0.1-ml sampling loop and injected

† Journal article no. 9618 of the Michigan Agricultural Experiment Station.

‡ Present address: Cawthron Institute, Nelson, New Zealand.

Reprinted from the *Soil Science Society of America Journal*
Volume 43, no. 5, September-October 1979
677 South Segoe Rd., Madison, WI 53711 USA

Methods for the Production and Use of Nitrogen-13 In Studies of Denitrification[1]

J. M. TIEDJE, R. B. FIRESTONE, M. K. FIRESTONE, M. R. BETLACH, M. S. SMITH, AND W. H. CASKEY[2]

ABSTRACT

Methods were developed for use of the radioactive isotope of nitrogen, ^{13}N, for short-term studies of denitrification. ^{13}N was generated by irradiation of water with 12 to 15 MeV proton beams from a sector-focused cyclotron. Under typical operating conditions of 0.7 to 3 μA beam currents for 10 min, the ^{13}N ionic species produced were NO_3^-, 75–90%; NO_2^-, 5–10% and NH_4^+, 0.5–25%. Traces of [^{13}N] N_2O and [^{13}N] N_2 were also produced. The measured yield varied from 2 to 16 mCi/10 min irradiation depending on beam current. Vacuum evaporation at high pH was used to obtain $^{13}NO_3^- + {}^{13}NO_2^-$ at > 99.8% purity, and high performance liquid chromatography (HPLC) was used to obtain $^{13}NO_3^-$ or $^{13}NO_2^-$ at > 99% purity. The HPLC system used a Partisil SAX anion exchange column eluted with phosphate buffer at pH 3.0 and was coupled to a coincidence NaI(Tl) detector for counting ^{13}N species in the effluent. Separation of NH_4^+, NO_2^-, and NO_3^- was achieved within 5 min. This system was used to monitor purity of ^{13}N substrates and for studies of dissimilatory nitrate reduction to ammonia. A gas chromatograph-proportional counter detector system was developed to separate and measure [^{13}N] N_2, [^{13}N] N_2O and ^{13}NO. Separation was by Poropak Q and Molecular Sieve 5A columns and was achieved in 5 min. Denitrification rates and products of soils and bacterial cultures incubated in sealed flasks were monitored with this system. Continuous rates of [^{13}N] N_2 and [^{13}N] N_2O production were monitored using a differential trapping, gas stripping system. Soil slurries amended with $^{13}NO_3^-$ or $^{13}NO_2^-$ were stripped of gases by continuously sparging with helium. N_2O was collected in a liquid nitrogen trap. Nitrogen gas passed through this trap but was retained in a Molecular Sieve trap immersed in liquid nitrogen. ^{13}N gases collected in each trap were continuously counted by NaI (Tl) detectors. Linear rates of gas production were typically observed from 15 min after addition of the ^{13}N substrate to termination of the experiment after 1 to 1.5 hours. ^{13}N has the advantage in denitrification studies of allowing direct measurement of N_2, very sensitive short-term rate measurements, and isotope exchange experiments at low substrate concentrations.

Additional Index Words: nitrous oxide, nitrogen gas, soil nitrogen, metabolism.

Tiedje, J. M., R. B. Firestone, M. K. Firestone, M. R. Betlach, M. S. Smith, and W. H. Caskey. 1979. Methods for the production and use of nitrogen-13 in studies of denitrification. Soil Sci. Soc. Am. J. 43:709–715.

RESEARCH on nitrogen metabolism and the nitrogen cycle has been hindered by the unavailability of a radioactive isotope of nitrogen. An alternative is the use of ^{15}N enriched or depleted nitrogen; however, sensitivity is often a problem since the detection limit is relatively high and always a function of the total nitrogen content of the sample analyzed. This limitation has been particularly severe to the study of denitrification since the major product, N_2, cannot usually be measured without altering the natural atmosphere of the sample being studied. Since O_2 is the principal regulator of denitrification, this is an important limitation. Use of a radioactive isotope of nitrogen allows direct measurement of N_2 in any atmosphere. ^{13}N is the longest lived radioactive isotope of nitrogen with a half-life of about 10 min, which allows an experimental time of 1-2 hours and is adequate for short-term studies of denitrification.

Besides direct detection of N_2, the high specific activity of ^{13}N, 1.88×10^{10} Ci/g-atm, provides extremely high sensitivity over the short-term. Assuming optimal operating conditions the minimum detectable amount of ^{13}N is less than 2000 atoms (3.3×10^{-21} moles). This compares to 1×10^{-12} moles for ^{14}C or 7×10^{-9} moles for ^{15}N (assuming 99 atom % excess). This greater sensitivity of ^{13}N over ^{15}N is often of importance in denitrification studies since the denitrification rate is dependent on nitrate concentration. The large additions of $^{15}NO_3^-$-N required (often > 50 ppm) for stable isotope experiments can cause an artificially high denitrification rate and will alter the ratio of N_2O/N_2 (4). In contrast concentrations of only 10^{-8} ppm or less of $^{13}NO_3^-$-N are needed to measure denitrification rates.

Little is known about transient events in denitrification, especially the response to changes in moisture and thus oxygen content of soils. ^{13}N because of its high sensitivity is well-suited to investigation of such short-term phenomena. Classical methods have generally required 0.5 to 1 day before the first discernable results could be obtained. ^{13}N allows measurement of denitrification rates in freshly collected samples before any significant change in enzyme concentration can occur. Also because of the high sensitivity, isotope exchange experiments can be performed at low substrate concentrations (4).

^{13}N has been used in the medical sciences (2, 15) and for studies of N_2 fixation (10, 22). Recently its application to studies of denitrification was demonstrated by Gersberg et al. (6). The utility of ^{13}N for denitrification studies is enhanced by the direct production of $^{13}NO_3^-$, which occurs when an H_2O target is used. This was first demonstrated by Lathrop et al. (9) and Gelbard et al. (5) in 1973 and has been successfully used in our studies.

In this paper we report on the procedures for production and purification of $^{13}NO_3^-$ and $^{13}NO_2^-$ and on rapid automated methods for measuring [^{13}N] N_2, [^{13}N] N_2O, ^{13}NO, $^{13}NH_4^+$, $^{13}NO_2^-$ and $^{13}NO_3^-$. These methods should also be useful for study of processes other than denitrification and for studies of transformations of other elements.

---

[1] Contribution from the Dep. of Crop & Soil Sciences, Dep. of Microbiology & Public Health, and the Heavy Ion Laboratory, Michigan State Univ., E. Lansing, MI 48824. Published as Journal Article no. 8928 of the Michigan Agric. Exp. Stn. This work was supported by NSF Grants DEB-77-19273 and PHY-78-01684 and USDA Regional Research Project NE-39. Received 3 Dec. 1978. Approved 3 Apr. 1979.

[2] Professor of Soil Microbiology, Assistant Professor of Chemistry and Heavy Ion Laboratory, and Graduate Students, respectively. Current addresses are: M. K. F., Dept. of Soils and Plant Nutrition, Univ. of Calif., Berkeley; M. S. S., Dept. of Agronomy, Univ. of Kentucky; and W. H. C., Inst. of Ecology, Univ. of Georgia.

Reprinted from the *Soil Science Society of America Journal*
Volume 43, no. 6, November-December 1979
677 South Segoe Rd., Madison, WI 53711 USA

The Influence of Nitrate, Nitrite, and Oxygen on the Composition of the Gaseous Products of Denitrification in Soil

M. K. Firestone, M. S. Smith, R. B. Firestone, and J. M. Tiedje

Vol. 91, No. 1, 1979 BIOCHEMICAL AND BIOPHYSICAL RESEARCH COMMUNICATIONS
November 14, 1979 Pages 10-16

NITRIC OXIDE AS AN INTERMEDIATE IN DENITRIFICATION: EVIDENCE FROM NITROGEN-13 ISOTOPE EXCHANGE

Mary K. Firestone[a], Richard B. Firestone[b], and James M. Tiedje[c]

[a]Dept. of Soils and Plant Nutrition, [b]Lawrence Berkeley Laboratory, University of California, Berkeley, CA 94720 and [c]Dept. of Crop and Soil Sciences, Dept. of Microbiology and Public Health, Michigan State University, E. Lansing, MI 48824

Received October 8, 1979

SUMMARY: Label exchange studies were used to investigate the role of nitric oxide as an intermediate of denitrification in Pseudomonas aureofaciens and Pseudomonas chlororaphis. The $[^{13}N]N$ from $[^{13}N]NO_2^-$ readily exchanged with pools of added, nonlabeled NO, with 54% of the $^2[^{13}N]N$ appearing in a pool of 7.2×10^{-3} atm NO in P. aureofaciens. These results suggest that NO is either an intermediate in the reductive sequence or is in rapid equilibrium with an unidentified intermediate.

INTRODUCTION:

Denitrification, the use of nitrogen oxides as electron acceptors during anaerobic respiration, occurs in a number of genera of bacteria. This process can be of significant agronomic importance because it converts the biologically available ionic forms of N (NO_3^- and NO_2^-) to gaseous products N_2 and N_2O. It has been commonly accepted that denitrification occurs via the following sequence of intermediates (1):

$$NO_3^- \rightarrow NO_2^- \rightarrow NO \rightarrow N_2O \rightarrow N_2$$

Currently, however, there is uncertainty as to the role of NO in the reductive pathway (2,3,4) and this uncertainty has been enhanced by ^{15}N tracer studies in Pseudomonas aeruginosa (2). In this paper we report the results of ^{13}N tracer studies using two denitrifying strains and discuss the compatability of these findings with several proposed pathways.

METHODS:

Pseudomonas aureofaciens (ATCC 13985; assigned to Pseudomonas fluorescens biotype E by Stanier, Palleroni, and Doudoroff [5]) was obtained from the American Type Culture Collection and Pseudomonas chlororaphis (assigned to Pseudomonas fluorescens biotype D [5]; from the strain deposited with ATCC as 17809) was obtained from G. E. Becker, University of Iowa. These organisms

0006-291X/79/210010-07$01.00/0

Proceedings of the International Conference on Nuclear Physics, Berkeley, California, August, 1980.

Nuclear Physics A354 (1981) 157c-172c. © North-Holland Publishing Co., Amsterdam

SPIN EXCITATIONS IN NUCLEI

G.F. BERTSCH

Cyclotron Laboratory and Dept. of Physics
Michigan State University, East Lansing, MI 48824

Abstract: The recent progress in the study of nuclear spin excitations is reviewed. The (e,e') measurement of the giant M1 state in ^{48}Ca and the systematics of the giant Gamow-Teller state seen in the intermediate energy (p,n) reaction give a clear picture of the spin-dependent dynamics. The effective interaction strength is consistent with previous knowledge of the nuclear force. However, the excitation strengths are much smaller than shell-model theory predicts. This may be understood at least partially by considering additional hadronic degrees of freedom.

Introduction

There has been great progress in the last few years in the study of spin excitations, and at this conference there are several significant contributions. For a long time, there was only one nucleus whose spin properties we really knew, namely ^{12}C. Now for the first time we have measurements of the spin excitation strength in magic nuclei with spin-unsaturated j-shell closures. The best example is ^{48}Ca, where there are recent measurements both of the M1 strength by electron scattering[1]), and of the strength of the Gamow-Teller operator $\sigma\tau_-$ by charge exchange reactions[2]). With such excellent quality data we can with confidence infer the properties of the residual interaction. We can also see a pattern emerging, with the spin operator becoming strongly quenched in nuclei.

Before I go into any detail on the interpretation of the experiments, I would like to remind you qualitatively what is learned. Measurement of the M1 strength tells us the degree to which spins are unpaired in the ground state. The excitation energy tells us the effective spin-spin interaction, which then should be usable to predict many other features of the spin degrees of freedom, such as higher multipoles, and interactions with spin-dependent probes such as pions.

M1 strength

According to the shell model, the M1 strength should be concentrated in a single particle-hole state for a closed shell nucleus with spin-unsaturated j-shell closures. The measurement on ^{48}Ca is particularly welcome for this reason. The experimental result is that the strength is indeed concentrated, in a state at 10.23 MeV excitation. This is seen in the data of Fig. 1.

The excitation energy of the ^{48}Ca M1 state is close to what is expected theoretically. I want to show you this in some detail, because there has been some controversy about ^{208}Pb, as to where in energy the state should be. In the simplest theory, the excitation energy is due to the single particle energy of the $(f_{5/2}f_{7/2}^{-1})$ configuration, together with the residual interaction. The single-

Proceedings of the International Conference on Nuclear Physics, Berkeley, California, August, 1980.

Nuclear Physics A354(1981)375c-394c. © North-Holland Publishing Co., Amsterdam

NUCLEAR COLLISIONS AT INTERMEDIATE ENERGY

David K. Scott

National Superconducting Cyclotron Laboratory
and
Departments of Physics and Chemistry
Michigan State University
East Lansing, Michigan 48824, U.S.A.

Abstract: Intermediate energy nuclear collisions in the energy region from approximately 10 to 200 MeV/u are discussed. Their importance in providing conceptual links between low and high energy processes is emphasised. The production of spectator fragments, of a participant or localised hot zone and of composite light particles by coalescence can already be discerned at 15 MeV/u. The transition from fusion in central collisions to explosive reactions also appears to take place at fairly low energies. Intermediate energy studies may be useful in relating low energy microscopic theories of TDHF, direct and multistep reactions to the macroscopic approaches such as nuclear hydrodynamics.

1. Introduction

Largely as a result of developments in accelerator technology, the study of nuclear collisions has been focused on two decades of incident energy: from 1 to 10 MeV/u by the numerous electrostatic and cyclotron accelerators throughout the world, and from 200 to 2000 MeV/u by modifications to existing synchrotrons. It has, however, become clear that the intervening decade from approximately 10 to 100 MeV/u contains important transitional features, a fact emphasised by the intense activity in the construction of intermediate energy accelerators. Some of the recently completed and proposed machines with their approximate energy domains are shown in Fig. 1, along with the characteristic physics expected. In the transitional region, the collision speed surpasses both the sound velocity and the intrinsic Fermi velocity. Instead of a mean field description, one may find that the mean free path of nucleons becomes short before nuclei lose their cohesiveness; hydrodynamic features may therefore come into play. On the other hand the energy is not so high

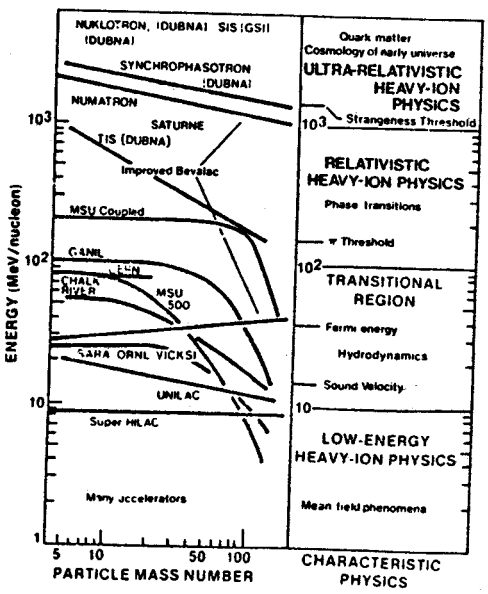

FIG. 1. The energy regions and possible characteristic physics covered by recently constructed and proposed heavy-ion accelerators. In cases where several machines cover similar ranges, only one representative line is shown.

Proceedings of the International School on Nuclear Structure

(Alushta. April 14-25, 1980)

NUCLEAR COLLISIONS AT INTERMEDIATE ENERGIES

D.K. Scott

National Superconducting Cyclotron Laboratory

Michigan State University

East Lansing, Michigan 48824

and

Département de Physique Nucléaire

C.E.N. Saclay

BP. No2, 91190 Gif-sur-Yvette

Introduction

The study of heavy ion reactions at intermediate energies, which we loosely define between 10 and 200 MeV per nucleon, has for sometime been recognized as important for providing links between low energy concepts and the superficially different approaches of relativistic heavy ion collisions. In this energy region, the average excitation increases beyond the characteristic intrinsic particle energies (≈30 MeV), with a concommittant diminution of the importance of quantal effects and an increased relevance of classical behaviour. Instead of a mean field description, one may find that the mean free path becomes short before nuclei lose their cohesiveness; hydrodynamic features may then come into play. From the perspective of general physics, the field of intermediate energy collisions is likely to be very interesting. One is neither in a quantal or a classical situation, neither in the one-body nor the two body extreme, neither close to the adiabatic nor the sudden regime. The explanation of phenomena in this region may therefore require the development of new theoretical approaches.

Through historical accident, the evolution of accelerators over the last decade has bypassed this interesting energy region. As indicated[1] in Fig. 1.1,† many accelerators exist around the world with energies up to 10 MeV/nucleon. In the early seventies, speculations about new states of matter at high densities spurred the development of high energy heavy ion beams on

†For clarity some of the illustrations in this paper have been redrawn from the originals. Reference should be made to the original literature for precise quantities.

ОБЪЕДИНЕННЫЙ ИНСТИТУТ ЯДЕРНЫХ ИССЛЕДОВАНИЙ

Дубна 1980 Д4-80-385

Reprinted from

PROGRESS IN PARTICLE & NUCLEAR PHYSICS

Vol. 4, *pp.* 5–93

Towards Relativistic Heavy Ion Collisions "By Small Steps Towards the Stars"

DAVID K. SCOTT

Nuclear Science Division, Lawrence Berkeley Laboratory, Berkeley, California 97420

INTRODUCTION

The study of relativistic heavy ion collisions began in the Heavens and that may well be where it will end. Almost thirty years ago the foundation of current approaches to high energy interactions between nuclei were laid, when in the primary cosmic radiation components with $Z > 2$ were discovered (Freier, 1948). At roughly the same time theorists were led by the properties of the nucleon-nucleon tensor force to speculate that the familiar saturation of nuclear density might be overcome and that tightly bound collapsed nuclei might occur in nature (Feenberg, 1946). Today there are many more speculations on the possible phases of nuclear matter under extreme conditions of temperature and pressure, and these speculations are being sharpened by the study of relativistic heavy ion collisions with accelerators at energies up to a few GeV/nucleon (for recent reviews of the field, see Goldhaber, 1978; Nix, 1978; Webb, 1978; Bock, 1978). Nevertheless, for a long time to come, the interactions generated by ultra relativistic cosmic rays in the atmosphere will constitute our only source of information on hadronic matter at very high energies of 10^6–10^9 GeV and beyond (Gaisser, 1978). In order to portray this unity between the cosmic and man-made accelerators, I show in Fig. 1.1 the Bevalac inside the exploding matter of the Crab Nebula. This is a symbolic illustration of the universal interest throughout the whole of physics in the collision of structured objects, especially insofar as they can be explained in the context of a microscopic theory. It is likely, indeed, that the study of relativistic heavy ion collisions holds the greatest hope for ultimately reunifying elementary particle physics, nuclear physics and astrophysics.

The relevance of cosmological events to relativistic heavy ion collisions is both profound and practical. In Fig. 1.2 is shown the temperature reached in the nuclear fireball, formed when two heavy ions collide, for two assumptions about the hadronic mass spectrum (Glendenning, 1978). The curve labelled "experimental" corresponds to a mass spectrum containing the known particles whereas that labelled "Hagedorn" corresponds to the bootstrap hypothesis of an exponential growth of hadrons. In this model the temperature limits at 140 MeV which may have been observed (Laasanen, 1977), a temperature approaching the limit reached in the earliest recognizable moments of our Universe (Weinberg, 1977).

PERGAMON PRESS
NEW YORK · OXFORD · FRANKFURT · PARIS
1980

McGraw Hill Yearbook of Science and Technology (1980)

NUCLEAR PHYSICS

by David K. Scott

Nuclear physics

In the study of nuclear reactions induced by heavy ions, a major area of research is concerned with the formation of nuclei in extreme conditions, far removed from the normal states of nuclear matter. Nuclei are produced in states of very high angular

Reprint Series
16 May 1980, Volume 208, pp. 749-751

SCIENCE

Nitrous Oxide from Soil Denitrification: Factors Controlling Its Biological Production

Mary K. Firestone, Richard B. Firestone, and James M. Tiedje